MODELING AND SIMULATION OF CROWD EVACUATIONS IN TOXIC ENVIRONMENTS BY CONSIDERING THE IMPACT OF DOSAGE

A Thesis

by

NEIL ALVIN BACAL ADIA

Submitted to the Office of Graduate and Professional Studies of
Texas A&M University
in partial fulfillment of the requirements for the degree of

MASTER OF SCIENCE

Chair of Committee,	Konstantinos Kakosimos
Committee Members,	Luc Véchot
	Tingwen Huang
Head of Department,	Arul Jayamaran

August 2020

Major Subject: Chemical Engineering

ABSTRACT

In the event that control of process safety risk is lost, the effectiveness of mitigation barriers is paramount in reducing the consequences. When it results in an event such as a toxic gas release, a mitigation barrier that is present when humans are involved is emergency evacuation. The evacuation process is affected by various factors in such situations, which includes any physiological effects caused by exposure to the toxic gas. These symptoms have the potential to affect how humans make decisions or their ability to self-rescue. This presents a need for evacuation simulation approaches that account for toxic exposure effects in order to assist in the assessment of consequences in such scenarios.

This work involves the implementation of a dosage-based evacuation effects model based on the Toxic Load, which is an indicator of toxic injury. This level of toxic injury determines how fast or slow evacuating agents move compared to their desired evacuation speed. An algorithm that calculates the dosage accumulation rate depending on exposure time and concentration was implemented to determine the Toxic Load.

An advanced evacuation simulator, FDS+Evac, was modified to facilitate the implementation of the dosage effects model. A case study on a realistic building geometry was carried out, showing how the evacuation patterns of 30 people varied as a function of hydrogen sulfide concentration. The study showed that the typical results that come out of evacuation simulations (such as evacuation time) are not sufficient indicators of risk. Therefore, a contour plotting approach was developed to provide insights on consequences

(such as toxic injury) as well as plausible solutions to reduce aforementioned consequences. The contour plotting approach allows more effective planning of emergency response, as well as building design.

DEDICATION

This work is dedicated to my family and to those closest to my heart.

ACKNOWLEDGEMENTS

I would like to express my sincere gratitude to my committee chair, Dr. Konstantinos Kakosimos, for his guidance throughout. His ideas and insights have been indispensable throughout all aspects of this work. He has shown an incredible amount of patience and provided sound technical advice, which have both been invaluable.

I would also like to express my immense gratitude to Dr. Luc Véchot, who has entrusted me with this project, funded my studies, and provided me with countless opportunities to grow professionally during my time at the university. His encouragement, along with his meticulous scrutiny have both been tremendously helpful to this work.

Much appreciation also goes to Dr. Tingwen Huang for his collaboration, support, and encouragement in his role as a committee member.

I want to extend my thanks to Timo Korhonen and Dr. Randall McDermott who are part of the FDS+Evac development team and have continuously given me timely technical support throughout the duration of my work.

I would also like to thank my fellow students, the department faculty, and staff at Texas A&M University for being such a big part of this stage of my academic life.

Lastly, I would like to thank my parents, my brother, and my sister for their unparalleled love, support, and patience.

CONTRIBUTORS AND FUNDING SOURCES

Contributors

This work was supervised by a thesis committee consisting of Dr. Konstantinos Kakosimos [advisor] and Dr. Luc Véchot of the Department of Chemical Engineering and Dr. Tingwen Huang of the Department of Science.

All work for the thesis was completed independently by the student.

Funding Sources

This work was funded by the Mary Kay O'Connor Process Safety Center - Qatar industry consortium. In addition to the funding of this project, the consortium also provided the graduate assistantship, which covers tuition, fees, and stipend for the duration of the master's degree of which this thesis is a requirement of.

The consortium consists of representatives from Qatargas, QAPCO, QAFAC, ConocoPhillips, Qatar Shell, and the Gulf Organization for Industrial Consulting.

NOMENCLATURE

6MWD	6-Minute Walking Distance
6MWT	6-Minute Walking Test
AEGL	Acute Exposure Guideline Levels
CFD	Computational Fluid Dynamics
COPD	Chronic Obstructive Pulmonary Diseases
DNS	Direct Numerical Simulation
EPA	Environmental Protection Agency
ERPG	Emergency Response and Planning Guidelines
FDS+Evac	Fire Dynamics Simulator and Evacuation
FED	Fractional Effective Dose
H_2S	Hydrogen Sulfide
HSE	Health and Safety Executive
HVAC	Heating, Ventilation, and Air Conditioning
IDLH	Immediately Dangerous to Life and Health

IRIS	Integrated Risk Information System
LES	Large Eddy Simulation
NIOSH	National Institute for Occupational Safety and Health
OSHA	Occupational Safety & Health Administration
SLOT-DTL	Specified Level of Toxicity - Dangerous Toxic Load
SLOD	Significant Likelihood of Death
TL	Toxic Load
VLES	Very Large Eddy Simulation
WHO	World Health Organization

TABLE OF CONTENTS

Page

LIST OF FIGURES

Page

LIST OF TABLES

Page

1. INTRODUCTION

Accidents that involve toxic gas releases have always been regarded as having the potential to cause significant damage to both the environment and to human life. Large-scale industrial incidents such as those that occurred in Bhopal [1] and Seveso [2] are only some of the many grim reminders about the potentially catastrophic effects that these releases can inflict. It is of great importance, therefore, to understand, quantify, and control the risks related to toxic gas releases. One significant factor that can impact the outcome of any such scenario is the evacuation time, which may be limited by the physiological constraints that a toxic substance applies to an evacuating person.

Over the last three decades, evacuation models and simulators for pedestrian dynamics have been the subject of much study and development, resulting in various methodologies that were capable of simulating evacuation phenomena only through theoretical-based modeling. This is due to the lack of data resulting from actual, real-life evacuations. Based on the results obtained from these models, evacuation analyses can be carried out to predict the effectiveness of an evacuation scenario. Despite their success, none of the evacuation models encountered in publication were able to directly link the physiological constraints imposed by a toxic substance to evacuation performance during an evacuation scenario. The evacuation models that attempt to include toxic exposure only use such data to provide an estimation of fatalities without accounting for the direct effect of the toxic exposure on evacuation time. Results generated from the aforementioned analyses may have the tendency to underestimate the consequences of any given toxic release scenario due to the absence of a relationship between the effect of symptoms associated with toxic releases

and the ability of a person to self-rescue from such a release. Furthermore, the impact of building geometry design on evacuation is not addressed. Therefore, one of the aims of this project is to predict crowd evacuation behavior in toxic gas environments by accounting for:

- Dosage-based effects of toxic gas exposure on people's ability to evacuate.
- Complex interactions between humans during an evacuation scenario.
- Advanced crowd evacuation dynamics.

Accounting for these things allows for evacuation simulations to more accurately portray both physical and psychological aspects of crowd evacuation, which enables a better study of real-life evacuation scenarios in toxic gas environments.

Additionally, to be able to address the impact of building geometry design on evacuations in toxic scenarios, this project also aims to formulate a method of analysis that can help visualize and assess the evacuation performance of a given building design.

2. STATE OF THE ART

In order to carry out the required tasks, a literature search needs to be conducted covering all aspects of the project, which include the evacuation model and the toxic substance.

2.1 Evacuation Models

The goal of evacuation models is to be able to simulate the movement of people in an evacuation scenario, thus being able to predict evacuation patterns from a given physical geometry (room, part or all of a building, outdoor facility). They work by attempting to replicate tendencies in individual or crowd behavior that occur during an evacuation.

Evacuation models vary widely in their methodological approach, but their variations can be categorized by examining six main features of evacuation models, as described by Xiaoping et al. [3]

1. Approaches: The logical and/or mathematical basis behind the model. A combination of approaches may be used based on need.
2. Modeling of individuals/groups: Evacuating agents may have the same properties throughout the entire population (homogeneous) or may have variations in their properties as dictated by characteristics such as age, gender, psychology, and others (heterogeneous).
3. Model Scale: Approaches that account for individual interactions are considered on the microscopic scale, while those that consider interactions emerging from a group as a whole are considered on the macroscopic scale.

4. Space and Time: Evacuation models may be discrete or continuous in time and/or space.
5. Situations: Evacuation models may attempt to simulate evacuation in normal or emergency scenarios.
6. Typical Phenomena: Typical crowd behavior patterns that need to be replicated in a simulation.

Xiaoping et al. have identified seven approaches to studying evacuations, which are detailed in the following subsections. For purposes of this study, a suitable evacuation model would not only be able to replicate crowd behavior in emergency scenarios, but also be able to accommodate features of toxic exposure with relative ease without having to make excessive changes to the existing model.

2.1.1 Cellular Automata Models

Cellular Automata are representations of physical systems, idealized mathematically as a regular uniform lattice of "cells", where space, time and physical quantities are discrete. Physical quantities measured in Cellular Automata are represented by discrete numerical values. As the Cellular Automata evolve in discrete time intervals, the value in each cell is influenced by the values of those in neighboring cells at the previous time step. The degree to which these values are influenced are dictated by a set of defined "local rules" which vary from one application to another. This is done by approximating the governing differential equations of a physical system into finite differences and discrete variables [4].

The currently available Cellular Automata models fall into two main categories: those that are based on the interactions of agents and the environment surrounding them, and those that are based on the interactions of agents with each other.

Daoliang et al. [5] used a two-dimensional, Cellular Automata model in order to investigate the exit dynamics of agents in an emergency scenario. Motion of agents is determined by a simple set of local rules that use four main parameters: L, R, B and ϕ; the first three of which stand for the number of neighboring agents to the left, to the right and to the back of any cell. The final parameter ϕ is a measure of "panic", or eagerness to move and is determined based on a probability. The work demonstrated the phenomenon of "arching" around doorways, which negatively impacts evacuation time and is dependent on exit width and separation (for multiple exits).

Cellular Automata models were also used to investigate the effect of obstacles and exit positioning on evacuation time. Varas et al. [6] took advantage of the numerical discretization of Cellular Automata by using static "floor fields" to determine the motion of evacuating agents. Just as flow fields are determined as movement from regions of higher pressure to lower pressure, floor fields were defined in a similar manner. To ensure that all agents evacuate the domain, the cell(s) corresponding exit are assigned the lowest value. The further a cell is from the exit, the higher the value assigned to a cell. Certain cells can be assigned very high values to represent obstacles.

Building on models that used static floor fields, Kirchner et al. used dynamic floor fields as well to simulate agent-agent interactions that can account for phenomena such as lane

formation or herding. They also introduced the modeling of competitive and cooperative behavior [7] through the introduction of a friction parameter, which is a probabilistic measure of conflict resolution between agents that desire to move to the same cell at the same time. In this manner, Kirchner et al. were also able to identify three main behavior regimes (ordered, disordered, and cooperative) in which the friction parameter had varying degrees of dependence, thus leading to different evacuation times [8].

Fang et al. [9] used Cellular Automata models to explore the more flexible nature of human judgment in directional movement. This was done by allowing agents to step in the opposite direction in the event of a conflict (more than one agent trying to occupy the same cell) to optimize their movement toward their destination.

2.1.2 Lattice Gas Models

Lattice Gas models belong to a special category within Cellular Automata, featuring agents that are modeled as active particles, rather than being affected solely by the discrete physical values in neighboring cells. This allows complex modeling for movement in evacuation scenarios through the use of probability and statistics, producing more stochastic results. In most cases, the existing models use a "preferential direction" for movement of agents, which is the direction toward the exit for evacuation scenarios. Lattice Gas models have been used to examine the dynamics and characteristic behavior of movement through different building configurations.

Tajima et al. [10] used a Lattice Gas model to study the dynamic free flow and choking flow patterns through an exit doorway. They managed to reproduce distinct patterns that

are characteristic of evacuation crowd flows, such as flattening and arching at doorways. In addition, they studied the scaling behavior of crowd flow with respect to exit width, as well as the time to transition between crowd flow regimes.

Helbing et al. in 2003 [11] used experimental data from an evacuation carried out in a classroom, and used this data to calibrate evacuation model parameters. This would make evacuation models quantitatively reliable in addition to their ability to qualitatively reproduce evacuation patterns. Consequently, they were able to relate individual agents' evacuation times relative to their initial position, thus making it possible to evaluate the effectiveness of a building configuration.

Lattice Gas models have been used in conjunction with other models when studying evacuation dynamics. Song et al. [12] used a combination of Lattice Gas and Social Force models by using an additional grid to account for interaction forces between agents. When the grid cells of an agent overlap with those of another, they are interacting. The extent of interaction depends on the number of overlapping cells, as well as their relative position and the rules of the model itself. Social Force models are discussed in further detail in the following section.

2.1.3 Social Force Models

Some of the main concepts of social force were suggested by Lewin [13] in order to model more complex behavior, especially when dealing with changes in behavior. These changes are influenced by what are called, "social fields" or "social forces". Such forces may

emerge from changes in the environment or external stimuli, and according to one's personal aims and interests.

In the case of crowd evacuation, as studied by Helbing et al. in 1995 [14], social forces that affect agents arise from multiple sources:

1. *The desire to reach the destination as comfortably as possible:* Agents desire to take the shortest possible path towards the destination and will do so at a specific desired speed. The actual velocity of an agent may vary due to deceleration and/or avoidance processes that the agent has to undertake.
2. *The influence of other agents:* In most cases, agents have the desire to maintain a distance from other agents that depends on the density of agents in the surrounding area and the desired speed. An agent's "private sphere" can be modeled through repulsive effects in the immediate area around which the agent is occupying.
3. *The influence of walls and obstacles:* Agents may have the desire to maintain a distance from obstacles, and this is modeled in a manner similar to agent-agent repulsion.
4. *Attraction forces:* Agents may sometimes be attracted by other agents (such as friends) or objects (exit doorways), and can be modeled in the opposite manner to the repulsive forces.

The contributions from these forces were then combined into one working equation, as well as an additional fluctuating term to account for random variability in behavior.

Helbing et al. further improved upon the existing model in 2000 [15], adding a model for escape panic to replicate phenomena associated with such situations, which were summarized as follows:

1. People moving or attempting to move faster than normal.
2. Interactions between people becoming more physical (pushing).
3. Movement (specifically passing through bottlenecks) becoming uncoordinated.
4. Arching and clogging at exit doorways.
5. Building up of jams, and therefore enough pressure to harm physical structures.
6. Slowing down of escape due to injured/fallen people becoming 'obstacles'.
7. People tending towards mass behavior.
8. Alternative exits not being used efficiently or being overlooked altogether.

Modeling agents as spheres, Helbing used the following equation (based on a generalized force model) to describe the velocity of an agent as it varies over time:

$$m_i \frac{d\mathbf{v}_i}{dt} = m_i \frac{v_i^0(t)\boldsymbol{e}_i^0(t) - \mathbf{v}_i(t)}{\tau_i} + \sum_{j(\neq i)} \mathbf{f}_{ij} + \sum_{W} \mathbf{f}_{iW} \qquad (1)$$

Where: m_i - Agent mass

$\mathbf{v}_i$ - Actual agent velocity

v_i^0 - Desired agent speed

$\boldsymbol{e}_i^0$ - Desired agent direction

τ_i - Characteristic time

$\mathbf{f}_{ij}$ - Agent-agent interaction force

$\mathbf{f}_{iW}$ - Agent-wall interaction force

The right-hand side consists of terms that contribute to the agent's motion. The first term describes an agent's desire to reach a certain speed v_i^0 in the direction $\boldsymbol{e}_i^0$. The other terms are velocity-dependent interaction terms with other agents ($\mathbf{f}_{ij}$) and walls ($\mathbf{f}_{iW}$), which are described in more detail below:

$$\mathbf{f}_{ij} = \left\{A_i \exp\left[\frac{r_{ij} - d_{ij}}{B_i}\right] + kg(r_{ij} - d_{ij})\right\}\mathbf{n}_{ij} + \kappa g(r_{ij} - d_{ij})\Delta v_{ji}^t \mathbf{t}_{ij} \quad (2)$$

$$\mathbf{f}_{iW} = \left\{A_i \exp\left[\frac{r_{ij} - d_{iW}}{B_i}\right] + kg(r_{ij} - d_{ij})\right\}\mathbf{n}_{iW} - \kappa g(r_i - d_{iW})(\mathbf{v}_i \cdot \mathbf{t}_{iW})\mathbf{t}_{iW} \quad (3)$$

Where: r_{ij} - Sum of radii r_i and r_j

d_{ij} - Distance between two agents' centers of mass

d_{iW} - Distance between an agent's center of mass and a wall

$\mathbf{n}_{ij}$ - Normal direction from agent j to i

$\mathbf{n}_{iW}$ - Normal direction from wall to agent i

$\mathbf{t}_{ij}$ - Tangent direction from agent j to i

$\mathbf{t}_{iW}$ - Tangent direction from wall to agent i

Δv_{ji}^{t} - Difference in tangential velocity between agents i and j

A_i, B_i, k, and κ are constants.

The forces are analogous to one another - the first term acts as a repulsive interaction force, while the other two forces account for physical contact and are inspired by granular interactions. The first contact force term is a counter-compression “body force”, and the second is a “sliding friction force” that impedes relative tangential motion.

These Social Force models have been the basis of other works that investigated more complex evacuation behavior. Zheng et al. [16] used a neural network together with a social force model to simulate two different kinds of personalities - one displaying cooperative behavior, and another displaying independent behavior.

Despite the success of social force models in reproducing the most typical phenomena and producing realistic results [3], an underlying assumption on interactions was scrutinized by Henein and White [17], stating that granular behavior captures the interactions between passive particles. This means that the particles will behave in the same manner when exposed to the same flow conditions. Humans, on the other hand, react differently and thus the models have not accounted for non-homogeneity. They proposed a method of modelling force dynamically that exhibit its essential aspects, summarized as follows:

1. Force is *directed*, meaning that it must be in vector form due to its application from one agent to another in a specific direction.

2. Force is *consequential*, meaning that forces may affect agents in a way that causes them to lose control, such as being pushed in a certain direction or being injured.
3. Force *propagates*, meaning that it travels from one agent to another, is additive when transmitted along with other forces, and its effects occur over a certain length of time.
4. Force is *exerted purposefully*, meaning that agents have a choice on whether they exert force or not, depending on circumstance. For example, agents may push others when impeded or blocked from moving in their desired direction.

2.1.4 Fluid-Dynamic Models

Fluid-Dynamic models, as suggested by their name, emerge from descriptions of evacuating crowds having fluid-like properties. Henderson [18] found good agreement with Maxwell-Boltzmann theory when modeling a crowd as a mass of particles in the gaseous phase. Additionally, he observed several crowds of different types: students, pedestrians, and children. It was also found that the behavior of all three crowds had reasonably good agreement with Maxwell-Boltzmann theory - allowing for the approximation of crowd behavior using fluid dynamics as a basis.

Fluid dynamics was used by Mnasri et al. [19] to perform analysis on the flow of Hajj pilgrims walking across part of a bridge, in order to propose modifications to the bridge's design based on the predicted flow patterns. They used the Ansys Fluent Computational Fluid Dynamic code to resolve the governing equations of mass and momentum conservation, with the assumption of incompressible, laminar flow, and water as the fluid.

Hughes et al. [20] expanded on the subject by suggesting that crowds, while having many of the motion characteristics of a classical fluid, also have the ability to think. Thus, it was established that further advances in behavioral science are required to better describe the inhomogeneities in the flow, as well as the transition from macroscopic to microscopic (continuum to particle).

2.1.5 Agent-Based Models

Agent-Based models are computational models that develop social structures through the definition of rule sets that govern how agents interact with one another. Since the focus of these models are with these interactions, they are able to lend valuable insights into the mechanisms and preconditions for panic and jamming by incoordination [3]. This allows models to account for more complex characteristics of agents such as room geometry knowledge, herding, competitiveness, and obstacle avoidance behavior. Furthermore, their ability to model agents as individuals allows for the simulation of crowds with heterogeneous individuals.

Braun et al. [21] used a modified form of the Helbing Model [15], by extending it to give the agents the ability to recognize the identity of other agents. This was used in conjunction with another parameter called an agent's "Altruism" which is the likelihood of an agent to help other agents that it recognizes.

Pan et al. [22] used an Agent-Based model to simulate social behaviors during emergency evacuation scenarios. The model was able to model behaviors such as competitive, queuing, and herding, which was accomplished through the simulation of interactions

between autonomous agents. These agents are able to make their own decisions through sensors, decision-making rules, and actuators.

The strength of Agent-Based models lies in their ability to model individual agents to have unique behaviors; however, the trade-off is the high computational requirement when compared to other approaches.

2.1.6 Game Theoretic Models

Certain models may use the rules of Game Theory to model the decision-making process of agents. The game thus consists of the agents, each with its own set of possible actions, as well as all the utility payoffs that can possibly be obtained from each action. In Game Theoretic models, all of the agents conduct an assessment of the situation, after which they select the alternative that will lead to them having the maximum utility payoff.

Lo et al. [23] proposed a dynamic exit selection model based on Game Theory. In a multiple-exit scenario, this allows agents to make decisions based on what decisions other agents make that will minimize evacuation time. Thus, an optimal exit strategy exists for a given system, in which the payoff selected by each agent in its corresponding payoff matrix leads to a maximum.

Guan et al. [24] combined a Cellular Automata model with Game Theory , in which Game Theory is used in the conflict resolution process, when two or more agents compete for the same cell. Each agent who loses a conflict adjusts their strategy in a probabilistic manner. The model utilizes two notable parameters: the fear index, which represents an overall sense of panic - at large values, phenomena such as the faster-is-slower effect can

be reproduced; and a cost coefficient which represents the intensity of competition between agents.

2.1.7 Approaches Based on Evacuation Experiments with Animals

Due to possible ethical and legal constraints, experiments characteristic of genuine escape panic are difficult to conduct on humans, and therefore animals have been used to increase the understanding of escape panic dynamics. Based on the review conducted by Xiaoping et al. [3], two sets of experiments were performed.

Saloma et al. [25] conducted experiments to study the escape behavior of mice under panic conditions from a water pool towards a dry platform through an exit door. The results showed agreement with numerical predictions over short time durations.

Garcimartin et al. [26] conducted experiments using sheep to examine flow in bottleneck situations, as well as to shed more insight on clogging phenomena. The results demonstrated a reproducible phenomenon known as the “faster is slower” effect, which was also shown to occur in humans [27].

Experiments on ants were conducted by Altshuler et al. [28] to demonstrate the propagation of panic, resulting in herding behavior. The geometry consisted of a room with two symmetrically located exits, and under low-panic scenarios, both exits were being used with the same proportions. However, under high-panic scenarios, one of the exits was more heavily used than the other. Xiaoping et al. [3] reports that the results have good agreement with Helbing’s Model [15] that approximates human behavior. Despite

this, Xiaoping et al. [3] state that human beings have strong social consciousness that will greatly differ from mice and ants.

2.1.8 Approaches based on virtual reality and hypothetical-choice experiments

The use of virtual reality in experiments for evacuation modelling provides a safe method for experimenters to conduct scenarios that would otherwise be of high risk in real life. Experimenters have the freedom to design their experiment in terms of variables and constraints. Often times, the trade-off is in the psychological aspect of the experiments, such as their actual level of motivation to evacuate, among other things [29].

Tang et al. [30] utilized virtual reality experiments to determine the effectiveness of emergency signs in crowd evacuations. They were able to demonstrate that the absence of emergency signs increased evacuation time significantly. Furthermore, modifying how emergency signs looked also had an effect. They were also able to reproduce some escape behavior phenomena such as unsymmetrical usage of T-intersections.

2.1.9 Summary and Conclusions

Computationally efficient methods such as Lattice Gas and Cellular Automata models provide a relatively inexpensive alternative when studying general flow behavior. However, these models tend to lean towards homogeneity in the evacuating populace unless combined with other approaches to be used as a framework.

Fluid-Dynamic models focus on the macroscopic effects that evacuating crowds impose as a whole. Their flow behavior, which is approximated as a continuum, is more

appropriate when examining higher crowd densities as opposed to lower crowd densities where individual interactions become more significant [20].

Agent-Based models provide valuable insight into the heterogeneous behavior of individuals under evacuation scenarios. Furthermore, they can successfully capture emergent phenomena and describes a system of evacuating agents in a natural and flexible manner. However, despite the flexibility that they can afford, they are limited to the advancement of cognitive science and can potentially become quite a complicated task when modeling complex human behavior.

Social Force models are able to capture some of the observable phenomena due to agent-agent interactions that are modeled as forces. It must be noted that an underlying assumption of these models is that the agents exhibit granular behavior, which oversimplifies the way that agents interact with the environment and one another [17]. Despite the homogeneity that is implied by the granular behavior assumed in these models, it is worth noting that the force equations used in these models can afford a slight degree of heterogeneity, however possibly not sufficient to fully capture the complexities of human behavior.

Aspects of both Social Force and Agent-Based models provide a great degree of usefulness due to their conceptual applicability, making a combination of the two models advantageous in terms of application. The ability of Social Force models to translate environmental influences into forces makes for a practical framework for the implementation of toxic effects, the influence of which can also be translated into forces.

Furthermore, the heterogeneity offered by Agent-Based models can expand the response variability within a given evacuating population, whether the response is purely psychological or due to the effects of toxic exposure.

2.2 Dosage

The effects that an agent experiences when exposed to a toxicant are dependent on the time length of exposure and the concentration of toxicant at which the agent is exposed to. This relationship is also known as dosage. As an agent moves through a facility or part of a facility that is subject to a toxic gas release, they may experience varying exposure levels of toxicant that change over time and position. Consequently, their dosage needs to be evaluated continuously in order to keep track of the cumulative exposure and determine its effects on the agent's ability to evacuate.

2.2.1 Modes of Toxic Exposure

Upon exposure, toxicants can potentially enter the body through four routes:

1. Ingestion - Through the mouth
2. Inhalation - Through the respiratory tract
3. Injection - Through cuts in the skin
4. Dermal absorption - Through the skin membrane

Most of the time, injection and inhalation are effective routes of entry of a toxicant to the blood stream. In addition, they also tend to result in the highest peak concentration of toxicant in the blood in comparison with those of ingestion and absorption [31]. In the case of gaseous toxicants, the most common mode of entry into the human body is through inhalation.

2.2.2 Exposure

Haber's Law (Shown in Equation (4) below), states that the severity (or biological response) of a toxicant depends on the product between the concentration of the toxicant in air and the duration of exposure, also known as the Haber Product. Developed by German physical chemist Fritz Haber, this relationship along with its physical limitations have become the basis of exposure limits [32], [33].

$$C \times t = k = Constant \tag{4}$$

However, not all cases of chemical exposure injury are covered by this equation. Therefore, the concept of toxic load was introduced, which can represent toxic injury in a more generalized manner than the Haber Product and can be treated as a form of injury factor [34]. For inhalation of toxic gas, the corresponding toxic load is a function of concentration and time, usually expressed as follows [35].

$$Toxic\ Load = C^n \times t \tag{5}$$

Where: C - Concentration

t - Exposure time

n - Toxic load exponent (constant)

Following Equation 5, for oral chemical exposure, Equation 4 (Haber's Law) is obtained (n = 1). Other values of the exponent n were derived experimentally based on data. By conducting thorough analysis of previously published experimental data obtained through the testing on animals, ten Berge et al. [36] concluded that Haber's Law was not generally

obeyed for inhalation toxicity. Furthermore, it was concluded that a general rule for the value of the toxic load exponent n does not exist, meaning that it should always be obtained empirically from experimental data when both the concentration and exposure time are known.

Based on the work published by ten Berge et al. in 1986, Boris et al. [37] proposed an algorithm to evaluate the toxic load for a set of concentration-time points, using AEGL conditions for the onset of symptoms. Each category of AEGL or symptom and its exposure concentration range corresponds to a "band" that will be used in the calculation of the toxic loading rate. The integral is as follows:

$$TL(t) = \int_0^t TL_{rate}(t')dt' \tag{6}$$

$$TL_{rate}(t) \equiv \frac{dTL}{dt} = \frac{1}{t_b}\left[\frac{C(t)}{C_{t_b}}\right]^n \tag{7}$$

Where： t_b - Time corresponding to the upper limit of the band

C_{t_b} - Concentration at the upper limit of the band

$C(t)$ - Concentration at time t

The algorithm uses tabulated concentration and time points (such as AEGLs) and interpolates a power law function to cover points in between. The algorithm identifies which band(s) is/are affected by the given exposure concentration, which should either exceed or fall within the concentration bounds of a particular band. The rate of toxic load accumulation is calculated for a defined exposure. The toxic load is then obtained by using

the rate and the total exposure time. The output of the algorithm consists of numeric values between 0 and 1 for each symptom or band. A value of 0 at a band means that the current level of exposure makes no contribution to the onset of a particular symptom. A value of 1 at a band means that the corresponding symptom has been reached.

The algorithm presents some limitations, as discussed by Boris et al. in their work. The toxic load calculated by the algorithm does not differentiate between a certain level of exposure encountered at the beginning, middle, or near the end of the certain period. In addition, the model does not account for detoxification performed by the human body, which becomes significant when the concentration of exposure fluctuates, or is zero in between periods of exposure at high concentrations. Work was done by both Ride [38] and Yee [39] to account for this phenomenon using additional terms in the toxic load model. However, this is not likely significant for relatively short periods of exposure such as in evacuation processes unless the detoxification rate for a particular gas is high and can be accounted for.

2.3 Emergency Response

The assessment of emergency response strategies is vital and can lead to a minimization of consequences as a result of a toxic chemical release scenario. Two options for emergency response are available for consideration: evacuation of the facility or sheltering in place. Evaluating the outcomes of each strategy usually requires the comparison of the overall toxic dosage encountered by personnel to certain standardized criteria, which is further discussed in this section.

2.3.1 Emergency Response Planning Guidelines (ERPGs®)

ERPGs® are exposure limits developed by the American Industrial Hygiene Association Guideline Foundation's Emergency Response Planning Committee. They are derived primarily using acute toxicity data, and other sources of information when such data are unavailable. These guidelines are more suited for the general public and account for rare, unforeseen, short-term chemical releases. A description of the three ERPG levels are shown below [40]:

ERPG-1: The maximum airborne concentration below which nearly all individuals could be exposed for up to 1 hour without experiencing more than mild, transient adverse health effects or without perceiving a clearly defined objectionable odor.

ERPG-2: The maximum airborne concentration below which nearly all individuals could be exposed for up to 1 hour without experiencing or developing irreversible or other serious health effects or symptoms that could impair an individual's ability to take protective action.

ERPG-3: The maximum airborne concentration below which nearly all individuals could be exposed for up to 1 hour without experiencing or developing life-threatening health effects.

2.3.2 Acute Exposure Guideline Levels (AEGLs)

AEGLs are a set of threshold exposure limits published by the United States Environmental Protection Agency (EPA) and are developed for different exposure periods, for different levels of severity of toxic effects. AEGLs are divided into three levels, each developed for five exposure periods - 10 minutes, 30 minutes, 1 hour, 4 hours, and 8 hours. The three AEGLs and their physical descriptions are shown below [41]:

AEGL-1: the airborne concentration of a substance above which it is predicted that the general population, including susceptible individuals, could experience notable discomfort, irritation, or certain asymptomatic non-sensory effects.

AEGL-2: the airborne concentration of a substance above which it is predicted that the general population, including susceptible individuals, could experience irreversible or other serious, long-lasting adverse health effects or an impaired ability to escape.

AEGL-3: the airborne concentration of a substance above which it is predicted that the general population, including susceptible individuals, could experience life-threatening adverse health effects or death.

The AEGLs account for five exposure periods, whereas the ERPGs only account for exposures of up to hour. AEGLs also account for susceptible individuals (young, elderly, and those with compromised immune systems).

2.3.3 Immediately Dangerous to Life and Health (IDLH)

IDLH concentrations are those defined by the National Institute for Occupational Safety and Health (NIOSH) for various chemicals, defining safe exposure levels for exposure times of up to 15 minutes [31].

2.3.4 Specified Level of Toxicity - Dangerous Toxic Load (SLOT-DTL) and Significant Likelihood of Death (SLOD)

Both established by the UK Health and Safety Executive (HSE), SLOT DTL and SLOD are both used to determine the toxic load that produces a specific level of harm at a certain received dose. SLOT DTL is defined as the dose that results in the death of highly susceptible people and for a substantial portion of the exposed population requiring medical attention as well as severe distress to the remainder exposed. SLOD is defined as the dose that will typically result in 50% fatality (LD_{50}) of an exposed population, which is extrapolated from animal experiment data [42]. They are mainly used as an alternative to the Probit approach, which is described in Section 2.3.5.

2.3.5 Probit

Probit equations are usually represented in the form:

$$Y = k_1 \times k_2(\ln V) \tag{8}$$

Where: Y - probit value (ranging from 2.67 to 8.09 which represents fatalities of 1 to 99.9%) which is a measure of the proportion of individuals that might sustain damage.

k_1, k_2 - Constants

V - the intensity or concentration of hazard raised to an exponent n and multiplied by the duration of exposure.

The values of constants are provided by the Center for Chemical Process Safety and are based on data obtained from toxicological studies. These equations only account for the fatality rate as a result of exposure and not for any other symptoms or adverse health effects.

2.3.6 Summary

The guidelines discussed above provide criteria that allow for the evaluation of mitigation and emergency response strategies in the event of a toxic chemical release. However, each method has its own limitations. For example, the different ERPG and AEGL levels are defined in an obscure manner, making it difficult to draw deterministic conclusions about effects on crowd evacuation from a certain exposure. These methods do not fully account for the variance in the responsiveness of a given population; instead they try to generalize and capture as much of the population as possible. Therefore, until the descriptions emergency response guidelines are updated to reflect physical effects of toxic exposure in some form, toxicological studies will need to serve as the main reference point exposure concentration when establishing toxic effects.

2.4 Simulation Approaches for Evacuations in Toxic Environments

The following are simulation approaches that have been developed to attempt to describe crowd evacuations in toxic environments.

2.4.1 Traffic Evacuations under Toxic Release Conditions

Durak et al. [43] used an Agent-Based model to simulate the evacuation of an urban population in the event of a chlorine spill. The program models the behavior of drivers evacuating within an urban area. The objective of the study was to be able to optimize traffic light systems for random initial traffic and spill conditions that will result in a minimum amount of deaths and injuries.

The simulation evaluates the amount of chlorine exposure that drivers experience and assumes 7 air exchanges per hour inside a vehicle. The level of exposure is then compared to AEGL levels which will then be used to change a driver's behavior, depending on which level they are exposed to. Moreover, the exposure of pedestrians is evaluated, but only for AEGL-2 purposes, and the reasoning is discussed in more detail below. The definitions and descriptions of behavior changes are summarized as follows:

AEGL-1: the level at which 50% of people can detect the gas. Drivers become aware of the gas, are more likely to turn on their radios, and are more likely to learn more quickly about the instructions to evacuate. Pedestrians will reach AEGL-2 earlier than drivers and thus exhibit symptoms due to chlorine exposure. Drivers that see those pedestrians become more aware of the emergency.

AEGL-2: the level at which 50% of people are affected by the gas and in some way disabled. Drivers who reach this exposure level will stop their vehicles. They may potentially survive if their exposures do not reach AEGL-3. However, due to their idle position, they will experience continuous exposure to the gas and also block traffic.

AEGL-3: the level at which the gas is fatal to 50% of people. The simulation treats the car and driver the same way as AEGL-2 (immobile), but the driver is then considered as a fatality.

Other characteristic behaviors involve car following, awareness, and sense of urgency. Car following is simply a form of herding behavior commonly reproduced in many evacuation models. Awareness is a measure of a driver's decisiveness to evacuate, which is increased by either being in AEGL-1 (detecting the gas) or observing pedestrians being affected by AEGL-2 levels of exposure. Sense of urgency captures the effects of stress on the driver in a panic situation, and decays over time when not exposed to stress. Different drivers are affected in different ways, but sense of urgency generally increases due to awareness, effects of exposure, and even getting stuck in traffic. High urgency causes a driver's judgment to be impaired, causing them to break traffic rules, such as running red lights and driving in an opposing lane. Such decisions may result in traffic accidents (non-exposure related casualties). It must be noted that the study does not account for the specific physiological effects that chlorine exposure can impose, but instead uses simple rules upon reaching a certain exposure limit.

2.4.2 Evacuation Modeling Coupled with Dispersion Modeling

Wan et al. [44] studied crowd evacuations inside a subway station under a toxic gas release scenario. Together with a Social Force model for evacuation, they used a Gaussian Puff model to account for the change in concentration of a toxicant over time and position.

To account for injuries and fatalities as a result of toxic gas exposure, they marked 3 different areas to indicate severity based on concentration and proximity to release source: Lethal Area, Injured Area, and Flesh Wound Area. Based on the position of evacuating agents relative to these areas, their escape speeds were defined, and are summarized as follows:

Lethal Area: The speed of the agent is zero, and the agent is considered a fatality.

Injured Area: The initial speed of the agent is halved.

Flesh Wound Area: The agent's speed is set to 90% of its initial speed.

In any other location, the agent's initial speed is doubled in consideration of nervousness. However, the study only considers the concentration component of the dose and does not account for the time length of exposure. Furthermore, they have no scientific basis on the change in initial speed of evacuating agents with respect to their level of exposure.

Lovreglio et al. [45] developed a methodology to simulate the evacuation of a crowd under a toxic gas release while simultaneously accounting for an agent's dosage as they evacuate. Using the ten Berge modification of Haber's Law ($C^n \times t$), the dose was calculated using their proposed dynamic approach, in contrast to the static approach used

in previous studies. The static approach involves the assumption that the concentration is constant throughout the domain, as well as the assumption of agents being "stationary observers". The results are then generated by conducting a spatial analysis, from which the fatality rate is evaluated depending on the final average total evacuation time. The proposed dynamic approach involves the calculation of the dose which is dependent on the path that the agent chooses to take. This dose is evaluated through a curvilinear integral over the agent's path. The fatality rate is then obtained by using a standard probit model derived from published toxicological data. It must be noted, however, that this methodology follows the entire evacuation path before deciding an agent's probability of death rather than applying the effects of toxic exposure as an agent evacuates through the domain.

Liang et al. [46] developed a methodology that involves a Gaussian dispersion model for the toxic gas release combined with an Agent-Based model for evacuation. The basis of the model involves a "belief-desire-intention" process in which a balance is created between an agent's proactive goal and its reactions to the dynamic environment around it. The toxic effects of exposure are accounted by scaling a Toxic Concentration Time (TCt) to the Lethal Concentration Time (LCt) of the toxicant. This ratio is called the "Health Index" (H). They defined an agent to be seriously injured when its H value is between 0.5 and 0.8, and dead when H exceeds the value of 0.8. The approach was only used to account for mortality rate and does not account for any other symptoms or physiological effects.

2.4.3 Dosage-Based Evacuation Modelling

Nawayd in his work [47] coupled a dosage model with a physiological effect model and incorporated it into Helbing's Social Force Model [15] as a contribution term. The dosage model tracks agent dosage as they evacuate, and depending on the value of dosage, the evacuation velocity of agents is modified to reflect the symptoms they are currently experiencing.

The methodology was demonstrated using a simple evacuation program where an escape scenario from part of an administrative building was simulated at varying concentrations of hydrogen sulfide. It showed how the effects of toxic exposure impact the evacuation process. While the methodology is conceptually sound, there are ways in which it can be improved due to several limitations:

- The evacuation model used (Social Force Model) is heavily theoretical and not validated.
- The evacuation model used does not account for many complexities of human movement, such as agent rotation, heterogeneous escape behavior, and the demonstration of complex behavioral characteristics as seen in real-life evacuation scenarios.
- The evacuation model used is inaccurate under certain conditions, namely in situations where there is counterflow of agents, where agents do not actively react to oncoming agents to avoid collisions.

- The program used to implement the evacuation also lacks certain important features, such as support for multiple exits within a building.

The current study plans to build upon the dosage approach in order to overcome these limitations by using the coupled dosage and physiological models as a basis for implementing toxic effects, which will be incorporated into a validated evacuation model.

2.4.4 Reporting and Visualization of Results

In general, evacuation case studies report results such as evacuation time relative to any variable being studied: exit width [12], level of building familiarity [48], and specially-defined parameters [17]. Additionally, studies that aim to explore evacuation dynamics report results in terms of forces (Social Force model applications) [49] as well as evacuation velocities [50]. However, for scenarios in which toxic substances are involved, these results are not sufficient. In addition to the aforementioned, such studies have included in their statistics, the estimated number of fatalities and injuries [23], as well as monitored dose [46]. However, this was done outside the context of building geometry design and thus only works in a case-to-case basis. Furthermore, the past studies do not account for dosage-based effects, with the exception of the work done by Nawayd [47].

2.5 Simulation Tools for Crowd Evacuation

When simulating crowd evacuations, it is very important to be able to account not only for agents' movement throughout a building domain towards an exit, but also to account for the psychological aspects behind the evacuation process. This psychological aspect includes the complex interactions that occur between evacuating agents, such as competitive egress behavior, herding and following between certain groups of agents, and evacuation behavior considering an agent's familiarity with its surroundings (mainly exit locations). Furthermore, the ever-evolving demands of building design in recent years have resulted in building plans that are spatially complex both in layout and in shape. As a consequence, these layouts may produce crowd flows that are highly complex [51].

Consequently, simulation tools were developed that combined aspects of evacuation models that were discussed in Section 2.1 along with concepts from other fields of science in order to capture the complexities in human evacuation movement and interactions between humans in such scenarios. Furthermore, they were built to overcome limitations of standalone evacuation models that run into inaccuracies during certain crowd flow scenarios [52]. This section aims to provide a description of evacuation simulation tools and their capabilities, which will aid in the selection of the most suitable one for the purposes of this project, which is to include both dosage-based effects on evacuation, advanced crowd dynamics and complex human interactions.

2.5.1 Panic Simulator

The Panic Simulator, developed by Julian Schmidt and Alexander Spah [53] is a simple open-source simulation tool that uses Helbing's Social Force Model [15] as its method to describe agent evacuation behavior. The parameters of the Social Force Model can be changed according to preference, or even automatically within a given range for testing purposes. It represents agents as 2D circles that move within a 2D geometry, which can only accommodate one exit. Its advantage lies in its simplicity, however, it lacks the capacity to account for complex agent behavior and advanced evacuation dynamics.

2.5.2 SIMULEX

SIMULEX is a simulation package that aims to model the escape behavior of agents from highly complex building geometries [51]. It is able to represent these escape scenarios in a 3D space using 3D representations of walls, obstacles, and agents. SIMULEX uses a feature known as "distance mapping" to evaluate the optimal path that agents can take towards an exit. It combines this optimal path with values obtained for unimpeded evacuation velocity in order to simulate human movement. It represents agents as a three-circle representation similar to the one proposed by Langston et al. [54]. To account for evacuation dynamics, it takes into consideration the "inter-person distance" and uses it to modify agent velocities depending on how tightly packed a crowd is. SIMULEX also accounts for the overtaking of agents when two agents have enough of a difference of evacuation speeds, using a route deviation algorithm that first assesses whether there is enough room for overtaking to be possible before doing so.

2.5.3 Pathfinder

Pathfinder is an agent-based simulation tool that uses path following similar to that used in SIMULEX, which it calls “steering”. The simulation tool is capable of running in two different modes: steering mode, in which the movement algorithms naturally result in complex behavior such as plugging of exits and queueing; and SFPE (Society of Fire Protection Engineers) mode, in which walking speeds are controlled by crowd density and exit flows are explicitly specified as a function of door width [55]. Pathfinder represents agents as well as building geometries in 3D forms, by using a triangulated mesh. The path following algorithm in Pathfinder uses locally defined waypoints in between an agent’s current position and the location of their target exit, in order to re-calculate the path in case a more desirable path is found. Pathfinder is able to account for differences in building geometry knowledge through its seeking algorithm, which accounts for waypoints, rooms, and exits that agents can actively seek as they evacuate. Agents can be set to have varying degrees of escape behavior, such as agents actively maintaining a specific separation distance between each other and actively avoiding obstacles and walls. Pathfinder also assigns a priority level to agents to allow for different agent escape behaviors in terms of competitiveness. Agents with the same priority levels to each other will treat each other neutrally, while agents with higher priority levels than others will actively try and push against those agents, resulting in competitive escape behavior. Pathfinder utilizes a collision avoidance algorithm in order for agents to actively avoid collisions between each other or with walls.

2.5.4 FDS+Evac

Fire Dynamics Simulator (FDS) and Evacuation (EVAC), also known as FDS+EVAC, is an open-source simulation tool that allows simultaneous simulation of fire and evacuation processes. Developed by VTT Technical Research Centre of Finland, the evacuation model uses the social force model developed by Helbing et al. in 2000 [15]. The social force model was extended to include a rotational equation of motion, and the preferred walking direction is determined by generating a vector flow field using an incompressible fluid flow analogy. In addition, a counterflow collision avoidance model was used to prevent collisions from agents moving in opposite directions [52], which the Social Force algorithm fails to actively account for. The extended evacuation model is shown in Equations 9 and 10 , showing both translational and rotational degrees of freedom, respectively.

$$m_i \frac{d\boldsymbol{v}_i}{dt} = \frac{m_i}{\tau_i}(\boldsymbol{v}_i^0(t) - \boldsymbol{v}_i(t)) + \sum_{j(\neq i)} \boldsymbol{f}_{ij} + \sum_{W} \boldsymbol{f}_{iW} + \sum_{k} \boldsymbol{f}_{ik}^{att} \qquad (9)$$

Where: m_i - Agent mass

$\mathbf{v}_i$ - Actual agent velocity

v_i^0 - Desired agent speed

τ_i - Characteristic time

$\mathbf{f}_{ij}$ - Agent-agent interaction force

$\mathbf{f}_{iW}$ - Agent-wall interaction force

$\mathbf{f}_{ik}$ - Agent-environment interaction force

$$M_i(t) = \frac{I_i}{\tau_i}(\widetilde{\omega}_i^0(t) - \omega_i(t)) + \sum_{j(\neq i)} (\boldsymbol{R}_i \times \boldsymbol{f}_{ij}) \quad (10)$$

Where: M_i - Agent torque

$\boldsymbol{\omega}_i$ - Actual agent angular velocity

ω_i^0 - Desired agent angular speed

I_i - Agent moment of inertia

τ_i - Characteristic time

$\mathbf{f}_{ij}$ - Agent-agent interaction force

$\mathbf{R}_i$ - Radial vector

The model is able to reproduce many of the observable phenomena associated with crowd evacuations and also account for the change in agent velocity due to lowered visibility in smoke as well as the change in walking speed due to the inhalation of gaseous fire products. The effects of toxic inhalation are evaluated through a Fractional Effective Dose (FED) which is calculated for each agent. When the value of the FED exceeds unity, the agent is said to be incapacitated. The floor area taken up by an agent remains the same upon incapacitation, which implies that it remains standing up.

The exit selection model is based on a Game Theoretic model in which agents observe the actions of other agents and decide on which exit route to take. Their choice depends on

several factors such as how far they are from their target exit, the amount of anticipated congestion at their target exit, as well as exit visibility and how familiar they are with the building. As of the current version, there are four available types of agent behaviors, each with their own exit preference strategy.

2.6 Hydrogen Sulfide

Hydrogen sulfide is a colorless gas, with its odor being a characteristic. The majority of hydrogen sulfide found in the atmosphere is of natural origin, coming from sulfur springs and lakes. It is also found in the air surrounding geothermally active areas. Its relevance in the oil and gas industry stems from its presence in natural gas deposits, where concentrations of the toxic gas can reach up to 42% [56].

Perhaps one of the most representative and well-documented incidents in literature regarding the release of toxic hydrogen sulfide gas would be the Lodgepole incident that occurred in Alberta, Canada in December 1982. The blowout resulted in a leak of natural gas flowing at around 150 million cubic feet per day, with a hydrogen sulfide concentration of 28% (280,000 ppm), and causing 3 fatalities [57]. Other incidents involving high levels of exposure to hydrogen sulfide gas occurring in unconfined spaces, where natural ventilation was present. These incidents involved concentration levels of 100 ppm 6 hours after the incident [58] and above 700 ppm in the vicinity of the victims [59].

Hydrogen sulfide falls under the classification of irritant as well as chemical asphyxiant. Its primary mode of entry into the body is through inhalation and is transferred into the bloodstream through the lungs. Due to its density being greater than that of air, its absorption into the blood stream is rapid [60]. Its distinctive odor of rotting eggs is usually masked by the presence of propane or butane [35].

2.6.1 Toxicology

A toxicological study of hydrogen sulfide suggests that the exposure-response relationship for acute effects, particularly those affecting the Central Nervous System and the respiratory system, can be very steep. The US Environmental Protection Agency's (EPA) Integrated Risk Information System (IRIS) has reported that concentrations between 500 and 1000 ppm are enough to be life-threatening and can cause immediate unconsciousness. Furthermore, detection of such high concentrations of hydrogen sulfide was reported to be impossible, since high levels of hydrogen sulfide are capable of paralyzing the olfactory nerves [61].

The World Health Organization (WHO) [56] have detailed the major symptoms associated with exposure to hydrogen sulfide, which are dependent on concentration and are detailed as follows:

Table 1 Major Symptoms Associated with Hydrogen Sulfide Exposure, as Reported by the WHO.

Concentration Threshold (ppm)	Major Symptom
Starting at 11 ppm	Onset of conjunctival irritation due to the sulfide and hydrogen sulfide anions being strong bases.
Starting at 50 ppm	Serious eye damage occurs.
Starting at 150 ppm	Loss of olfactory sense due to olfactory nerve paralysis.
Starting at 320 ppm	Onset of pulmonary edema with a risk of death.
Starting at 530 ppm	Strong Central Nervous System stimulation with hyperpnoea and respiratory arrest.
Starting at 1000 ppm	Immediate collapse with paralysis of respiration.

In fatal cases of human intoxication, brain edema, degeneration as well as necrosis of the cerebral cortex and the basal ganglia have been observed.

Guidotti carried out an extensive study on human toxicity, with hydrogen sulfide as the focus [62]. He examined the effects of the chemical on the macromolecules in the human body as well as its effects on human biological processes. It was observed that the

exposure-response curve for lethality is extremely steep for hydrogen sulfide (shown in Figure 1), and that it does not follow Haber's Law.

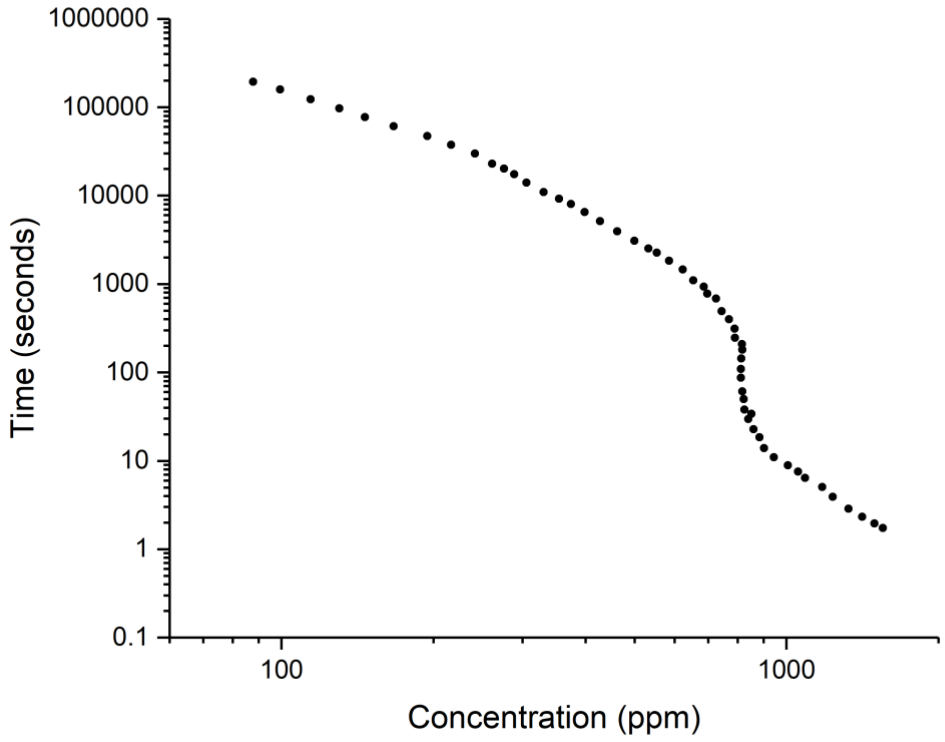

Figure 1 Lethality Exposure-Response Curve for Hydrogen Sulfide [62]. (Adapted)

The shape of the curve implies that the concentration of exposure plays a bigger role on the effects of exposure than its duration. A comparative study reports that the currently existing risk assessment models use a Toxic Load Exponent (n) between 1.36 and 4.36 but Guidotti claims that empirical evidence are strongly in favor of higher exponents. Guidotti

[63] also examined the concentration of exposure and its related physiological symptoms, shown in Table 2.

Table 2 Health Effects of Hydrogen Sulfide for Various Concentrations of Exposure, according to the work published by Guidotti [62]. (Adapted)

Concentration Range (ppm)	**Symptom**
0.01 - 3	Odor threshold (varies)
20 - 100	Eye and lung irritation, eye damage after several days of exposure
100	Olfactory paralysis
150 - 200	Severe eye and lung irritation
250 - 500	Possibility of pulmonary edema (especially at prolonged exposures)
500	Sudden unconsciousness, death within 4-8 hours
1000	Immediate collapse

2.6.2 Exposure Limits

Standards used in industry for exposure limits and emergency response guidelines with regards to hydrogen sulfide exposure are shown in Table 3 and Table 4.

Table 3 AEGLs for Hydrogen Sulfide.

Classification	10 min	30 min	1 h	4 h	8 h
AEGL-1 (Nondisabling)	0.75 ppm (1.05 mg/m3)	0.60 ppm (0.84 mg/m3)	0.51 ppm (0.71 mg/m3)	0.36 ppm (0.50 mg/m3)	0.33 ppm (0.46 mg/m3)
AEGL-2 (Disabling)	41 ppm (59 mg/m3)	32 ppm (45 mg/m3)	27 ppm (39 mg/m3)	20 ppm (28 mg/m3)	17 ppm (24 mg/m3)
AEGL-3 (Lethality	76 ppm (106 mg/m3)	59 ppm (85 mg/m3)	50 ppm (71 mg/m3)	37 ppm (52 mg/m3)	31 ppm (44 mg/m3)

The basis of these AEGL concentrations were based on a number of tests involving both controlled human and animal data are summarized as follows [41]:

AEGL-1: Ten adult volunteers with asthma were exposed by controlled inhalation of hydrogen sulfide for 30 minutes at a concentration of 2 ppm. Three out of ten complained of headaches, and eight out of ten experienced a nonsignificant increase in airway resistance.

AEGL-2: Rats were exposed to hydrogen sulfide at 200 ppm for 4 hours and experienced perivascular edema, from which an uncertainty factor of 3 was used to extrapolate from animals to humans.

AEGL-3: Rats were exposed to increasing concentrations of hydrogen sulfide were monitored, and the highest concentration causing no mortality after a 1-hour exposure was used as the basis.

Table 4 ERPG Tiers for Hydrogen Sulfide.

ERPG Tier	Concentration (ppm)
ERPG-1	0.1
ERPG-2	30
ERPG-3	100

The National Institute for Occupational Safety and Health (NIOSH) reported the Immediately Dangerous to Life and Health (IDLH) concentration for a variety of chemicals, which are considered safe for a 15-minute exposure. The reported IDLH concentration for hydrogen sulfide was 100 ppm.

Most of the toxicological reviews reported on hydrogen sulfide exposure symptoms provide an insight on the important concentration levels for industry awareness. However, the effects related to the time length of exposure are not covered extensively and a clear exposure-response relationship for hydrogen sulfide exposure symptoms (other than lethality) was not found.

2.6.3 Hydrogen Sulfide Symptoms and Effects on Evacuation Performance

Understanding how the symptoms of exposure affect the physiological and psychological features of human evacuations will allow for successful modeling of evacuation processes under toxic gas releases. The effects of the symptoms can then be translated into evacuation-related properties, such as evacuation speed or other parameters. A set of studies performed by Bhambhani et al. involved exposing exercising humans (both male

and female) to hydrogen sulfide concentrations of up to 10 ppm [64]–[68]. The test subjects were monitored for certain biological data before and after the experiment: Heart Rate, Blood pH, Oxygen Consumption, Carbon Dioxide Production, Expired Ventilation and Respiratory Exchange Ratio, Power Output and Lactate Levels. Their measured Power Output would be useful since it could be related to the average speed of a person. However, data for Power Output only exists in one paper in which the test subjects were exposed to a controlled concentration of up to 5 ppm [66]. In this exposure range, hydrogen sulfide did not cause any decrease in the power output but instead resulted in a non-significant increase in power output at concentrations of 0.5 and 2 ppm.

Fiedler et al. [69] exposed 74 healthy adults to hydrogen sulfide concentrations of 0.05, 0.5 and 5 ppm and had them complete some tasks in order to further understand the sensory and cognitive effects of acute hydrogen sulfide exposure. It was reported that increased anxiety was observed, which increased with exposure and was related to irritation due to odor.

Annegarn et al. [70] conducted tests on patients with Chronic Obstructive Pulmonary Disease (COPD), that involve the standard 6-minute walk test, or 6MWT. Examples of COPD include emphysema, chronic bronchitis, refractory asthma, and certain forms of bronchiectasis. Their walking characteristics were monitored using an accelerometer and compared to those of healthy people. The COPD patients were reported to show an altered walking pattern during the test compared to the healthy subjects, which could explain (to some extent) the lower 6-minute walking distance (6MWD) of the COPD patients, who

walked 26.2% less. However, it was concluded that the connection between the altered walking pattern and the walking distance is still unclear.

Stevens et al. [71] conducted an experiment to assess the reliability of 6MWTs that are usually performed on a treadmill, by seeing if it would result in a significant difference from walking in a hallway. This is because it was noted that people usually perform better in corridors because of their familiarity with them. 21 test subjects were asked to walk both on treadmills and corridors for six minutes. It was observed that their distance covered in hallways was much greater (around 100 ft more) than that on treadmills. The average walking speed in hallways was consequently reported to be greater (0.99 m/s) compared to the average walking speed on the treadmills (0.8 m/s).

Swerts et al. [72] conducted a similar comparison between hallway and treadmill tests for COPD patients, using 11 patients walking for 2, 6, and 12 minutes. It was also concluded that due to their familiarity with walking in corridors, they performed more efficiently. Therefore, the more appropriate testing method for COPD patients would be in corridors.

For more severe exposures, the physiological and psychological effects of symptoms such as pulmonary edema need to be examined. Pulmonary edema is a condition in which excess fluid builds up in the lungs and collects in the air sacs. According to toxicological studies by Gorguner et al. [60] and Guidotti [62], pulmonary edema can be developed as a result of hydrogen sulfide exposure, either immediately or up to 72 hours later. The symptoms of acute pulmonary edema are summarized as follows [73]:

- Extreme shortness of breath or difficulty breathing (dyspnea) that worsens with activity or when lying down.
- A feeling of suffocating or drowning that worsens when lying down.
- Wheezing or gasping for breath.
- Cold, clammy skin.
- Anxiety, restlessness or a sense of apprehension.
- A cough that produces frothy sputum that may be tinged with blood.
- Blue-tinged lips.
- A rapid, irregular heartbeat (palpitations).

These symptoms seem to have the potential to significantly impair the ability of a person to walk, but the extent of effect is unclear. This is because of the lack of availability on data related to severe exposure effects, as limited by ethical issues. Therefore, key inferences have to be made from these studies in order to provide an estimate for the effects of high exposures on the evacuation process.

2.7 Summary and Conclusions

Despite the numerous approaches and methods that were developed to simulate the evacuation process, gaps in knowledge still exist between toxic gas exposure and its effects on the evacuation process. The most concerning of these is the physical effect of exposure on evacuation velocity, which is essential for evacuation simulations.

There have not been any experimental studies that provide direct links or relationships between the toxicological effects or symptoms and their impact on decision making as well as the physical ability to evacuate. The available toxicological data is only useful in terms of the exposure-response relationship for mortality as a result of hydrogen sulfide exposure, and not for other symptoms.

The only suitable alternative to experimental data apart from guesswork is to rely on connections made between evacuation modelling and toxicological studies that have been performed for other purposes with the aim to obtain an approximation for toxic effects on the evacuation process. Emergency response guidelines to toxic release may be used to study crowd evacuations, but at their current form they are not specific enough in their description to draw conclusions regarding exposure effects on evacuation.

The usefulness of evacuation models such as Social Force and Agent-Based Models along with their implementation in advanced evacuation simulation tools allow them to be set up as a framework that can successfully account for toxic effects in relevant evacuation scenarios, due to the practicality of the force aspect of Social Force models and the flexibility of Agent-Based models. There exists a variety of simulation tools that can be

deemed suitable for this work, which will be chosen depending on availability as well as the capability to simulate evacuations in toxic gas release scenarios as completely as possible.

3. MOTIVATION AND SCOPE OF WORK

The aim of this work is to predict crowd evacuation behavior under toxic gas conditions by accounting for dosage effects as well as advanced evacuation behavior. Evaluating the consequence of an evacuation under toxic release scenarios requires a solid understanding of not only the social dynamics of the evacuation process, but also an understanding of how the toxic environment affects both the physical and psychological behavior of each evacuating agent. The latter can be achieved through the dynamic monitoring of each agent's toxic dosage. Through the dosage, it is possible to determine which symptom each agent will be experiencing at a certain time-step.

In this work, a simulation package will be selected based on the availability of models that are of relevance to the topic at hand: a Computational Fluid Dynamics (CFD) package, an Evacuation module, and capabilities for Heating, Ventilation, and Air Conditioning (HVAC) calculations. The focus of this study is on the evacuation process, and thus simplifications will be used in the other areas, taking the form of a worst-case scenario (Constant, uniform gas concentration, no HVAC operation). However, the availability of integrated dispersion modelling packages will be advantageous in future works.

The toxic load algorithm that was proposed by Boris et al. [37] will be used to determine the dosage experienced by each evacuating agent. Therefore, the extent of toxic injury can be determined and can also be associated to the various symptoms that result from exposure.

In addition, the toxic effects of hydrogen sulfide exposure will be accounted for in the form of adjusted evacuation velocities, which have been determined through toxicological studies found in literature. The source code of the chosen simulation tool will be modified to accommodate all of these changes.

The principles behind both Social Force and Agent-Based models can be taken advantage of due to the practical applicability of their concepts in terms of translating toxic effects into evacuation behavior. Social Force models are able to treat toxic gases and the effects of exposure to toxic gases as external influences that can affect an individual's ability to evacuate. Agent-Based models are highly applicable, not only in making the psychological evacuation behavior heterogeneous but also any response to a particular exposure level of toxic material. However, such data is limited due to experimental constraints and so any Agent-Based models used will act as a framework for such an implementation, should the appropriate data be available.

It should be noted, however, that the dosage effects model used in this work is not necessarily limited to Social Force and Agent-Based model approaches. The dosage model at its current state exists to cater to those models, but for practicality reasons. This is due to the current availability of simulation tools that can be built up to account for all aspects of evacuations in toxic gas environments. Apart from this constraint, the dosage model should be adaptable to any form of evacuation model that incorporates force and/or velocity in any form.

This model will be tested using a realistic evacuation scenario as a case study, and the results will be analyzed using various data visualization methods that can effectively communicate the level of hazards relevant to crowd evacuations in toxic environments.

4. METHODOLOGY

Satisfying the objective requires implementing a dosage-based methodology for calculating evacuation velocities under toxic release conditions into a currently existing crowd evacuation program, and then assessing the toxicity-related risks in an evacuation scenario. Currently existing and dedicated evacuation software allows the methodology to thrive under a complex evacuation environment, which involves additional interactions and more parameters besides the base evacuation model equation. The implementation involved getting familiar with the software and taking advantage of the improved dynamics to provide a clearer picture of the evacuation process. Furthermore, the dynamic Toxic Force term can be calculated as a function of evacuation symptoms, which are in turn a function of toxic dose, which provides a physical analogy for the variations in evacuation velocity.

4.1 Dosage Monitoring, Toxic Load, and Physical Effects

The monitoring of toxic dosage is the main driver for the evaluation of each agent's escape velocity in relation to the amount of toxic gas they are exposed to. The change in velocity is the way through which the model expresses the symptoms that each agent experiences. The dosage model used in this study is adapted from the one used in Nawayd's [47] work.

For dosage monitoring, the algorithm proposed by Boris [37] was selected for time-dependent dosage calculation, and was used exclusively for its sequence of calculation steps. The AEGL onset levels were instead replaced by the concentration levels

corresponding to symptoms due to hydrogen sulfide exposure, according to a study by Guidotti [62], [63] as well as from OSHA [74].

The values for concentration levels were interpolated from the values found in the works performed by Guidotti and OSHA, assuming that the dose-response relationship found for all symptoms follow the same behavior as that of the lethality curve.

This assumption was based upon the similarity of trends between Guidotti's exposure-response curve and AEGL-x curves, shown in Figure 2.

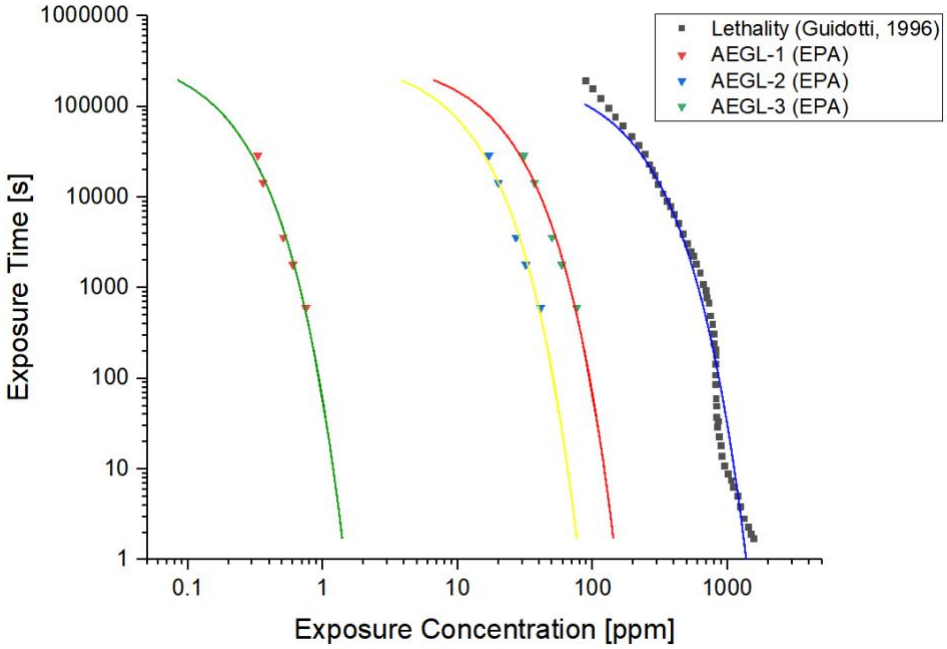

Figure 2 The Trend of AEGL-x Curves Compared with the Trend of the Lethality Curve Provided by Guidotti [62].

However, based on Salem [75], AEGLs are “rightfully conservative” and will “overestimate consequences” due to their “misapplication of toxicological concepts”. Thus, rather than using the AEGL curves as basis for dosage monitoring, curves for certain symptoms related to hydrogen sulfide exposure were formulated. The curves would then follow the same behavior as that of Guidotti’s curve, shown in Figure 3 and Figure 4. The values for the concentration levels related to exposure symptoms to hydrogen sulfide are summarized in Table 5 below.

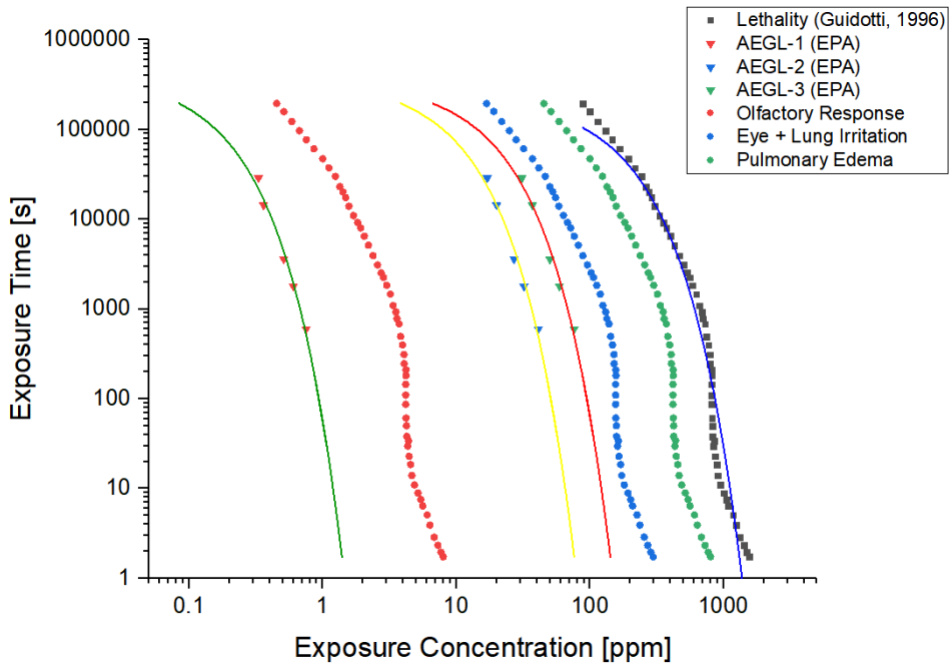

Figure 3 Various Exposure-Response Curves for Hydrogen Sulfide Exposure. Note the Over-Estimation of the AEGL Curves Compared to the Values for Exposure Symptoms.

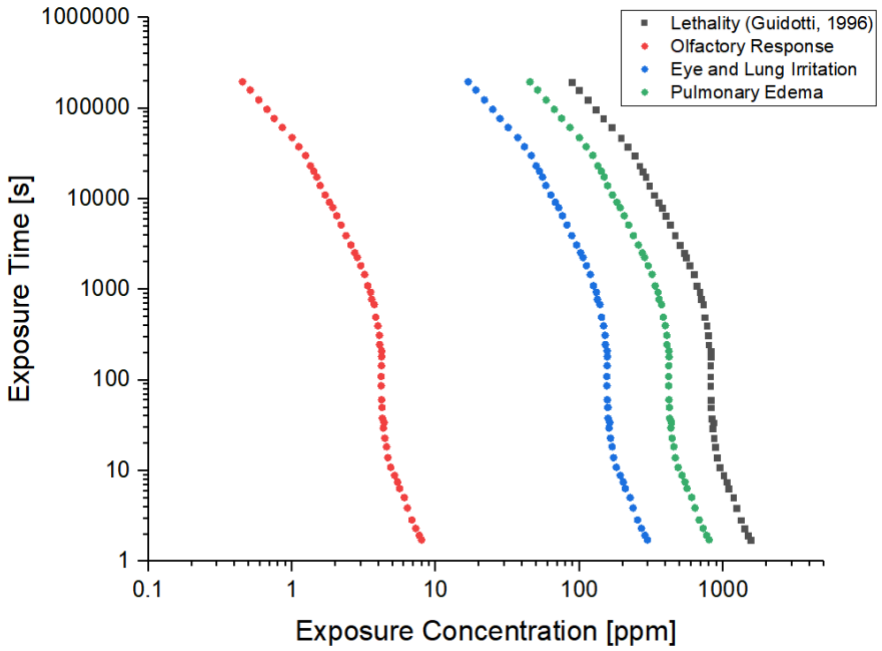

Figure 4 Exposure-Response Curves Used in this Study to Evaluate Effects for the Various Symptoms for Hydrogen Sulfide Exposure.

Table 5 Concentration Ranges for Symptoms of Hydrogen Sulfide Exposure.

Symptoms/Effects	Concentration levels (Source)
Slightly above odor threshold where odor becomes more offensive	3-5 ppm (OSHA) [74]
Slight conjunctivitis ("gas eye") and irritation of respiratory tract after 1 hour of exposure Altered breathing, drowsiness after 15-30 minutes of exposure at 100 ppm	50-100 ppm (OSHA) [74]
Prolonged exposure may cause pulmonary edema	250-500 ppm (Guidotti) [62]
Knockdown	500 ppm (Guidotti) [62]

The exposure-response curve between the time of 10 seconds and 1000 seconds (equivalent to about 17 minutes) is nearly linear, which was noted when keeping track of symptom exposure limits, since a large number of evacuation scenarios are expected to be within that time range. From the prior information and the experimental studies conducted by Fiedler et al. [69] which concludes that humans exhibit increased anxiety when exposed to 5 ppm of hydrogen sulfide, it was decided that scaling down the curve for the smell response to 5 ppm exposed for 10 seconds.

Guidotti [62] concluded a concentration range of 150-200 ppm for severe eye and lung irritation, while OSHA provides a range of 50-100 ppm during a 1 hour exposure period for slight eye and throat irritation. This would result in a dose-response curve in the allotted 10-1000 second time frame for concentrations between approximately 150 and 180 ppm.

An assumption was also made that once the upper limit for the symptom band related to Pulmonary edema was exceeded, agents will experience knockdown. The meaning of "prolonged exposure" causing pulmonary edema was not explicitly defined, and thus the assumption of the worst case comes into play. It was decided to use the shortest exposure time and highest concentration to use for pulmonary edema to set in. The outputs of the modified Toxic Load algorithm are summarized in Table 6 below according to the symptom they represent.

Table 6 Interpolation Data for Dose-Response Curves.

Symptoms	**Minimum Exposure Rate**
Smell	5 ppm for 10 seconds
Eye and Lung Irritation	100 ppm for 45 minutes
Pulmonary Edema	500 ppm for 10 seconds

These dose-response curves was be used in order to calculate an accumulated Toxic Load. The algorithm of Boris also calculates the rate at which toxic exposure symptoms are being

approached. This is known as the Toxic Loading Rate and is calculated at specific time intervals for any given exposure-response relationship. These loading rates are added up over the course of an agent's exposure which will determine their extent of toxic injury. Every exposure curve leading up to a specific symptom will be treated as a separate "band", through which the extent of toxic injury can be estimated for multiple symptoms as a consequence of exposure to one toxic substance.

The bands selected for hydrogen sulfide exposure are the three symptoms illustrated above, as they are the best starting point to provide the most dynamic response to exposure in terms of evacuation behavior. The modified toxic load algorithm therefore provides 3 levels of Toxic Load output, according to the symptom onset as shown below in Table 7.

Table 7 Exposure Bands Representing the Various Symptoms of Hydrogen Sulfide Exposure.

Symptoms	**Exposure Band**
Smell	$0 < TL \leq 1$
Eye and Lung Irritation	$1 < TL \leq 2$
Pulmonary Edema	$2 < TL \leq 3$

The dosage-dependent Toxic Load is the basis for the effect of toxic exposure that is expressed as a change of evacuation velocity. According to studies performed by Fiedler and Bhambhani [64]–[69], hydrogen sulfide exposure at very low concentrations of about

5 ppm caused heightened anxiety and had no negative impact on an agent's physical abilities. This should cause an agent to move faster due to discomfort upon detecting the distinguishable smell of hydrogen sulfide. Due to this, it was assumed that the maximum evacuation speed that an agent can reach for this symptom is 2 m/s, halfway between normal walking speed (1.35 m/s) and jogging speed (around 2.68 m/s).

The severe eye and lung irritation symptoms belong to the 2nd band, and the respiratory irritation symptoms can be likened to those experienced by patients suffering from Chronic Obstructive Pulmonary Disorders (COPD). Stevens et al. [71] conducted 6 Minute Walking Tests (6MWTs) on such patients, resulting in maximum evacuation speeds between 0.92 and 1.03 m/s, which can be estimated as 1 m/s.

There is still a lack of literature data for pulmonary edema patients' walking speeds or other relevant pieces of information. However, the effects associated with pulmonary edema include extreme shortness of breath and feelings of suffocation, which are significantly more severe than lung irritation. Therefore, it can be assumed that once an agent experiences pulmonary edema, their evacuation speed will reach zero, effectively incapacitating them. It is also expected that their evacuation speed would decrease between the onset of the last two symptoms.

The modified evacuation velocity related to the onset of a symptom can be referred to as the symptom speed (v^{00}), and is summarized in Table 8 below as a function of dosage.

Table 8 Toxic Load as a Function of Symptom Speed.

Toxic Load	**Symptom Speed** ($\boldsymbol{v^{00}}$)
$TL = 0$	1.35 m/s
$TL = 1$	2 m/s
$TL = 2$	1 m/s
$TL = 3$	0 m/s

It is important to note that the relation between symptoms and toxic dosage remains unclear as a result of little to no existing data. Therefore, the symptom speeds mentioned above are assumed to be those that agents experience when their corresponding symptom has reached its maximum effect. In that case, symptoms are applied at the beginning of each band, after which increased toxic exposure would cause evacuation speeds to decrease in a continuous manner until the symptom's maximum effect has been reached.

In order to achieve this, non-linear curve fitting functions were proposed for the various exposure bands relative to the symptom speed in order to achieve continuity as opposed to sudden step changes in evacuation speed. These are shown in Figure 5 below.

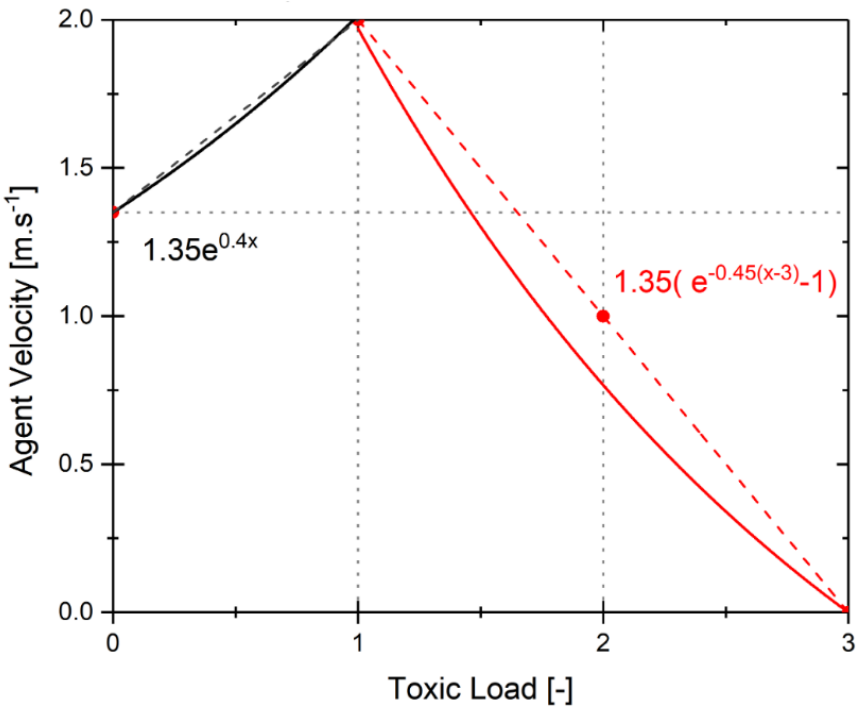

Figure 5 Continuous Functions Proposed for Velocity in terms of Toxic Load [76]. (Adapted)

The continuous functions for the main thresholds of toxic injury are summarized in Table 9 below.

Table 9 Table Summarizing the Continuous Functions Proposed in Figure 5.

Toxic Load	Symptom Speed (m/s)
$TL = 0$	$Desired\ velocity\ (1.35\frac{m}{s})$
$0 < TL \leq 1$	$v^{00} = 1.35e^{0.4TL}$
$1 < TL \leq 2$	$v^{00} = 1.35(e^{-0.4(TL-3)} - 1)$
$2 < TL < 3$	$v^{00} = 1.35(e^{-0.4(TL-3)} - 1)$
$TL = 3$	0

4.2 Implementation in FDS+Evac

The dosage methodology was implemented into FDS+Evac, which is one of the simulation tools discussed earlier and is originally designed for crowd evacuations during fire scenarios FDS+Evac is an open-source simulation tool developed and maintained by the VTT Technical Research Centre of Finland which builds on the FDS fire simulation module developed by the National Institute for Standards and Technology (NIST), adding an evacuation module. FDS+Evac is written in the Fortran programming language, and is a complex program consisting of over 1000 subroutines and functions that attempt to simultaneously model fire and evacuation processes. In order to successfully carry out the implementation, it is important to identify the key working functions and subroutines that perform relevant processes or work with relevant variables. FDS+Evac is an open-source project and can be found on the NIST website at (https://pages.nist.gov/fds-smv/downloads.html).

4.2.1 Theoretical Basis

FDS+Evac works through coupled dispersion and evacuation models that exchange relevant information with one another. A general summary of the main stages of FDS+Evac functionality is shown in Figure 6 below.

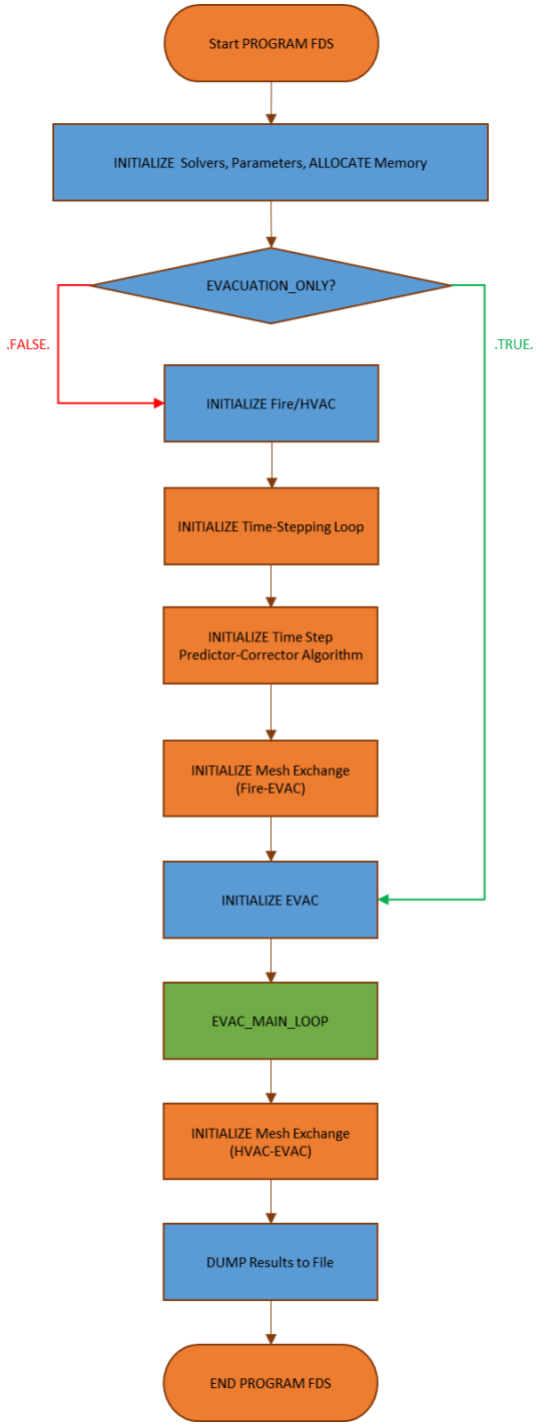

Figure 6 Main Stages of the FDS+Evac Program.

First, the dispersion model is run if the specified mode of simulation allows it. This involves numerically solving some form of the Navier-Stokes equations for thermally driven flows at relatively low speeds. The simulation geometry is discretized into a user-specified rectilinear mesh, on which the governing equations are also approximated. Multiple meshes are possible, but their use requires a specific set of conditions to be fulfilled. The numerical scheme used for CFD is an explicit predictor-corrector scheme, which results in second-order accuracy in time and space. It is capable of approximating turbulent flows using Large Eddy Simulation (LES), Very Large Eddy Simulation (VLES), and Direct Numerical Simulation (DNS) if the mesh is of an appropriate level of refinement.

Next, relevant information from the dispersion model is exchanged between the "fire" and evacuation meshes. This information includes variables such as soot density and concentrations of certain notable gases relevant to fires such as oxygen, carbon monoxide, and carbon dioxide. These variables affect the evacuation process in their own way, and these effects are quantified whenever available.

Following the Fire/EVAC mesh exchange, the evacuation model is run. The geometry once again is discretized into a user-specified rectilinear 2-dimensional mesh different from that of the fire mesh. A modified version of Helbing's social force model is used, which adds a rotational equation of motion as well as parameters related to anisotropy. Furthermore, it employs the concepts of agent-based evacuation models by introducing heterogeneous behavior through agent properties that can be adjusted to make each agent

react differently. EVAC guides agents to exits through a vector field applied to the evacuation mesh. This vector field is generated by using an approximate flow field solution for a two-dimensional incompressible fluid flow in the geometry, treating exit doors as an outlet boundary condition. This assumption holds better for larger crowd densities. For smaller crowd densities, wider paths will be more frequently used over narrower ones as a consequence of the assumption. Agent movement calculations are carried out using a modified velocity-Verlet algorithm. EVAC supports staircases to some extent; additional evacuation meshes are required for every floor added to the geometry. In scenarios with multiple exits, a Game Theoretic model is applied to assist agents in making decisions for which exit to choose.

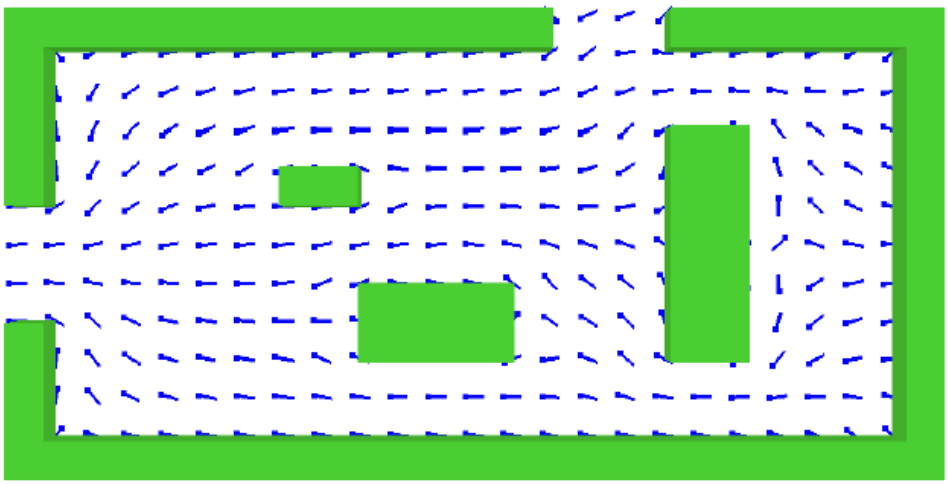

Figure 7 Illustration of vector flow fields used to guide agents to their chosen exit.

4.2.2 Evacuation Features

Agents possess properties such as position, torso and shoulder radii, and desired evacuation velocity. All these properties allow the equation of motion for each agent to be solved. Furthermore, these properties can be adjusted for each individual agent or group of agents, which introduces heterogeneous escape behavior typical of real-life evacuation scenarios. Agents are randomly placed throughout the domain within user-specified boundaries. The randomness feature can be disabled by users.

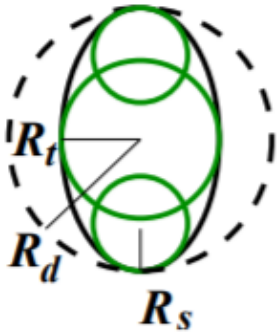

Figure 8 Illustration of an agent's shoulder and torso radii used to represent agent size in FDS+Evac.

Obstructions (including walls) can be added throughout the geometry to replicate real-life building geometries. The relative positions of these obstructions to evacuating agents influence the magnitude and direction of agent-wall interaction forces. Obstructions can be freely placed throughout the domain, but are restricted by shape and angle, as FDS+Evac does not support objects that do not have right angles.

Construction of geometry within the domain can be done through the input file, by manually specifying properties for each wall and obstruction contained in the domain. However, this is very time-consuming, especially when creating complex geometries containing multiple rooms and obstructions. Fortunately, a third-party tool called BlenderFDS, developed specifically for FDS+Evac, can be used to create such geometries without the unnecessary effort.

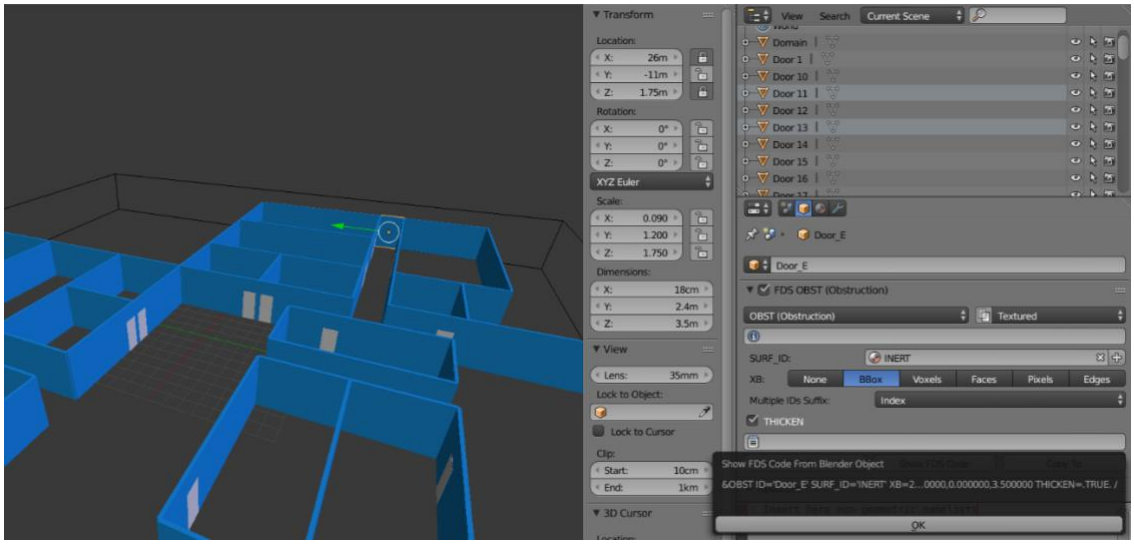

Figure 9 Screenshot of the BlenderFDS interface, showing the evacuation geometry and its corresponding FDS code.

Evacuation calculations require at least one exit to be present in the domain. Exits must be planar and placed onto the surface of a wall. The exit orientation relative to the domain must also be specified.

4.2.3 De-coupling of FDS from Evac

Running FDS+Evac means that both the CFD and the Evacuation models perform their calculations. However, it was found that on average, about 90% of the simulation time was attributed to the CFD calculations, which is significant compared to the time needed for the evacuation calculations. Therefore, de-coupling of the two processes would be beneficial in saving computational resources. Furthermore, modifications to the program will only affect the evacuation module, which means that only evacuation calculations are subject to change.

Based on Figure 6, if the EVACUATION_ONLY decision returns a value of .TRUE., then all the FDS (fire) calculations are skipped altogether and the program begins with the evacuation module. However, it is recommended by the developers to run both fire and evacuation calculations to be able to correctly generate the evacuation geometry as well as the output data files [52]. As a consequence, fire calculations cannot be avoided entirely. However, the fire calculation module generates output files after calculations are completed. If these output files are present in the working directory while the program is run, then the fire calculations are considered completed by the program. Thus, by running the fire calculations at least once per building geometry, an unlimited number of evacuation scenarios can be simulated given that the fire calculation output files from the first run are kept. This is illustrated in Figure 10 below.

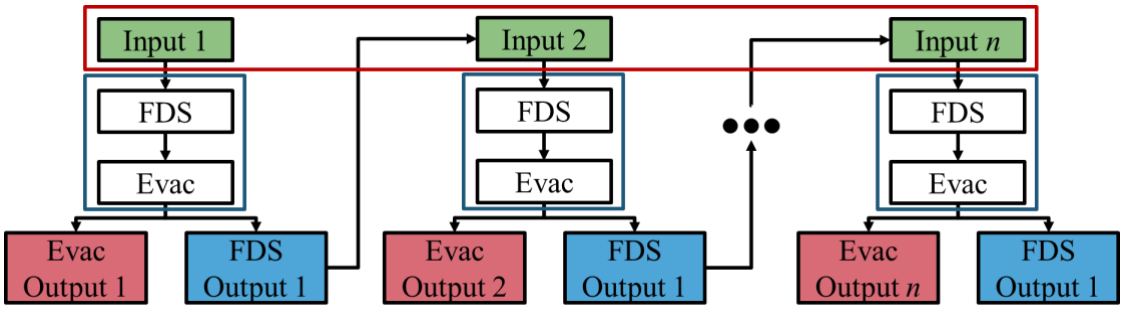

Figure 10 Illustration of how FDS output files will be used in calculations for computational efficiency.

Understanding the base features of FDS+Evac will provide a clearer picture on how to implement the effects of toxic dosage by taking advantage of similarities between the existing program and the proposed implementation.

4.2.4 Implementation of Toxic Effects Model

Each agent was assigned its own Toxic Load as a variable that was used by the program to modify evacuation velocities. An agent's Toxic Load was calculated by determining the loading rate for every time step, then summing them up for an agent's entire duration of exposure. The loading rate depends on the concentration of toxic gas, which is implemented in the model as constant at the current time of submission for this work. The agent velocities are changed using velocity modifiers that are currently being implemented in the source code of FDS+Evac. These modifiers are multiplied into the agent's desired velocity in order to obtain their final velocity after toxic effects have been accounted for.

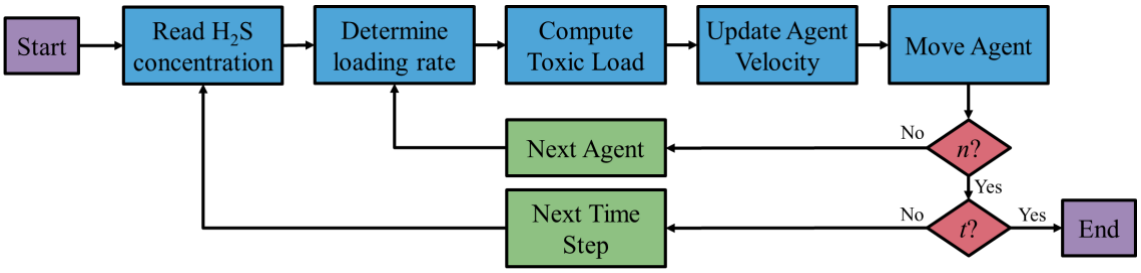

Figure 11 Algorithm of the Toxic Effects Model that was implemented into FDS+Evac for *n* agents and length of time *t*.

Agents' evacuation times are not recorded explicitly by FDS+Evac. Instead, the program keeps track of how many agents there are within the domain at any given time and subtracts one from the counter each time an agent finds its way to an exit. Furthermore, counters can be assigned to exits to determine the number of agents that decided to use a particular exit relative to other exits. A more accurate way of determining the exit time of agents is by looking at their recorded positions. FDS+Evac records agent properties at each time step and stops recording them when agents exit the domain. Thus, agent exit times were determined by looking at the time steps where the recording of agent positions stopped.

Newly implemented variables such as Toxic Load need to be recognized by the program as potential output variables. Therefore, the evacuation dump module was modified to allow Toxic Load values at each time step to be included in the output file at the request of the user.

5. RESULTS AND DISCUSSION

In order to test the implementation and provide more insights on the evacuation process using the advanced simulation capabilities of FDS+Evac, three case studies were performed. The first two case studies served as tests to investigate the effects of toxic load and exposure concentration on the evacuation process under relatively simple evacuation conditions. They also doubled as tests to verify the implementation of the methodology. The final case study was performed to simulate a realistic evacuation scenario under toxic release conditions and to use the results in order to develop a method of consequence analysis relevant to crowd evacuations in toxic environments.

5.1 Investigation of Effect of Toxic Load on Evacuation Time

The first case study was developed to demonstrate the effects of Toxic Load on evacuation velocity of agents. The case was run several times using different assigned values of Toxic Load for each agent. The values for Toxic Load were selected in a manner that would provide results for each stage of an agent's velocity variations as their dosage increased.

The setup was performed for 4 agents in a 10.8x10.0x2.4m domain (illustrated in Figure 12) with 2 exits. The simulation was allowed to run sufficiently long enough for all agents to exit the domain (if possible). Evacuation times were recorded for each agent during each run.

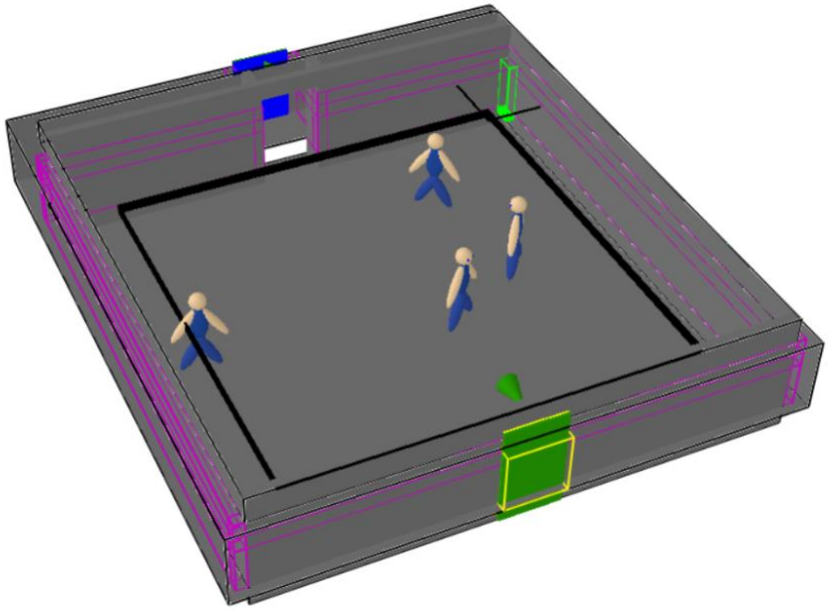

Figure 12 Screenshot of the simulation setup used to run the first test case.

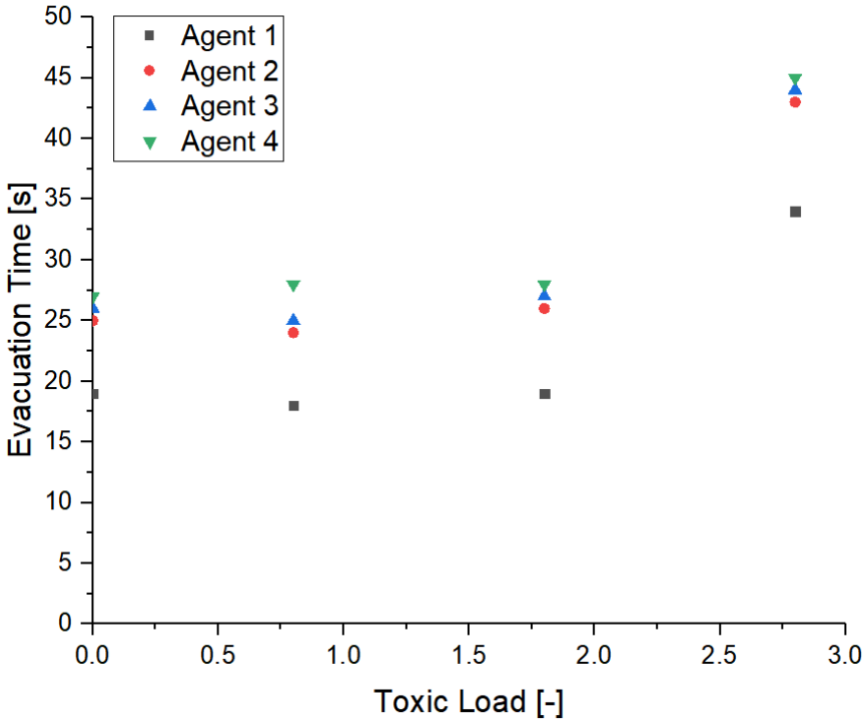

Figure 13 Variation of exit times as a function of Toxic Load for the first case study.

As seen in Figure 13, agents experienced a slight initial decrease in evacuation time before increasing as the Toxic Load increased. This is consistent with the increase in velocity associated with panic at low dosage, and then the decrease in velocity associated with symptoms due to higher exposure levels.

5.2 Effect of Exposure Concentration on Evacuation Time

The second case study was developed to investigate the effect of the exposure concentration on the evacuation time of agents through the Toxic Load Algorithm as it represents the impact of accounting for toxic exposure effects.

A simple setup was created consisting of a 100m long corridor with 1 agent beginning at one end, and the exit located on the other end. The simulation was allowed to run sufficiently long enough for all agents to exit the domain (if possible). Evacuation times were recorded for each agent during each run.

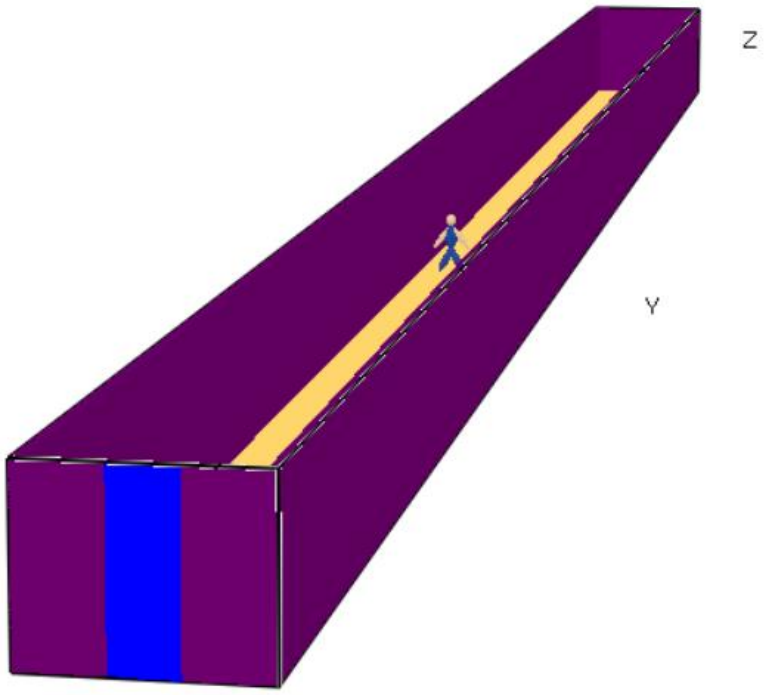

Figure 14 Screenshot of the simulation setup used in the second case study.

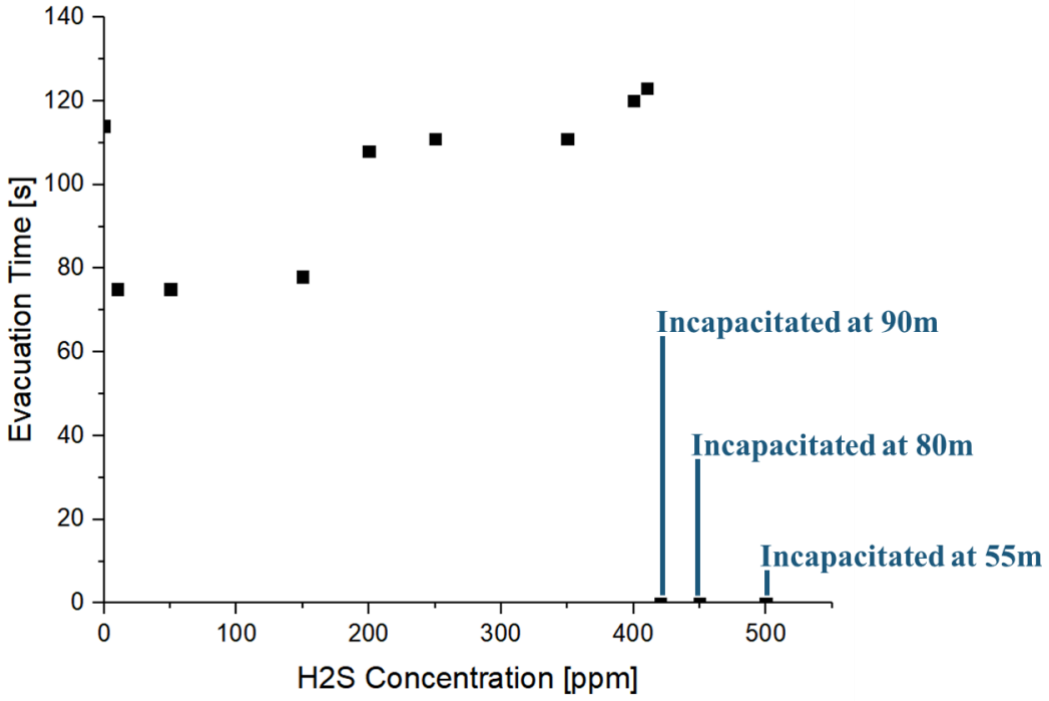

Figure 15 Variation of exit times as a function of H_2S concentration.

As Figure 15 shows, it takes about 110 seconds for an agent to reach the exit under normal conditions. Raising the hydrogen sulfide concentration to 10 ppm results in about a 30% decrease in evacuation time. However, in evacuations taking place in more complex building geometries and with multiple agents, there will be other factors affecting the evacuation time such as contact forces from other agents arising from clogging at exits or bottlenecks. This is more often observed in agents that move faster and is known as the "faster is slower" effect discussed in Section 2.

Higher concentrations cause agents to slow down due to them beginning to experience the 2nd symptom (eye and lung irritation). This leads to a gradual increase in their evacuation

time as the dosage rate increases and causes them to experience the 2nd symptom in a shorter amount of time.

When the concentration reaches much higher values, the agent experiences even higher increased evacuation times before becoming incapacitated due to the 3rd symptom (pulmonary edema) reaching its full effect. This test demonstrates how different levels of exposure contribute to changes in evacuation time due to changes in dosage rate that cause agents to experience different symptoms.

5.3 Effect of Exposure Concentration on Evacuation Performance in a Realistic Evacuation Scenario

5.3.1 Geometry

A realistic building geometry adapted from an actual building layout was created using BlenderFDS. The domain is 52 meters long and 52 meters wide. The building consists of 17 rooms, 2 open indoor areas, 2 short corridors, and 2 longer corridors. The building has 2 exits (shown as white arrows in Figure 16), one on the north side and one on the east side, both 2 meters wide. All of the smaller rooms open up into the open indoor areas, while the larger rooms open up into the longer corridors which contain the exits.

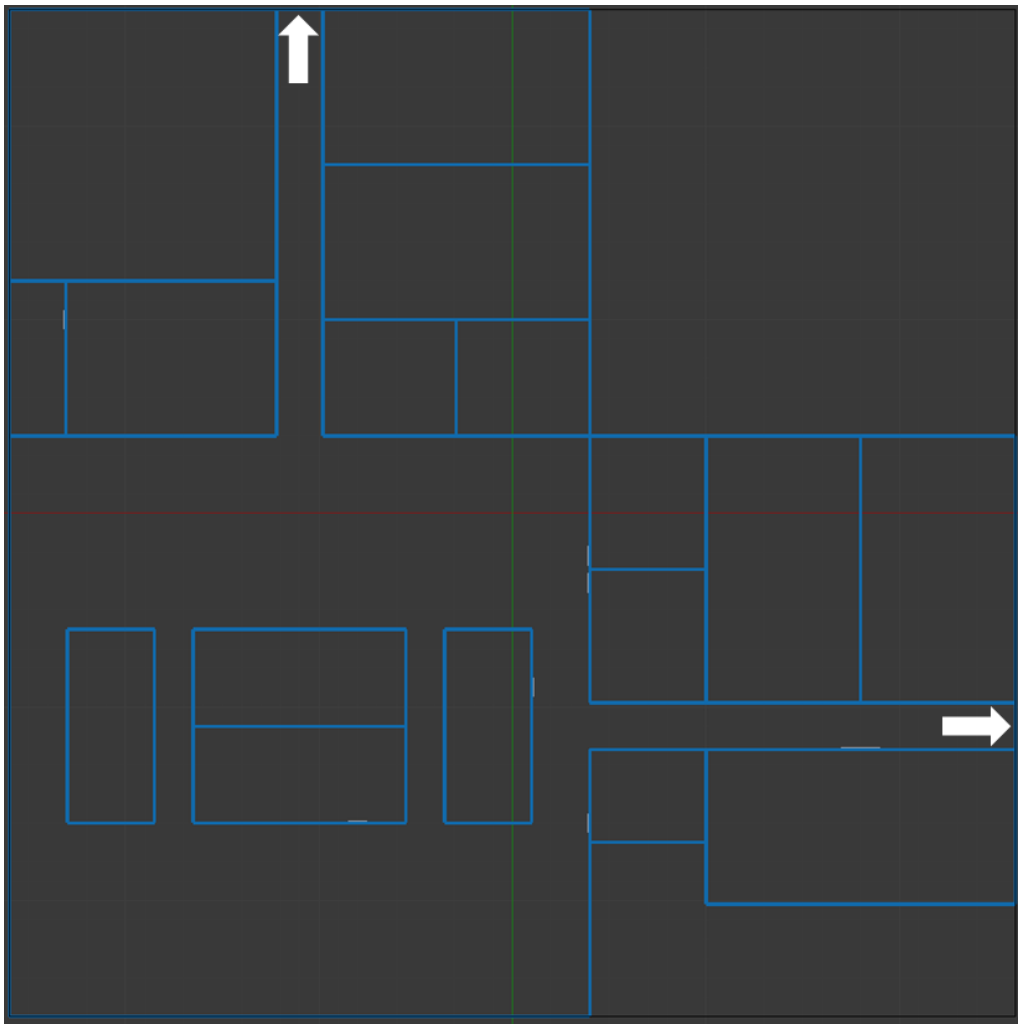

Figure 16 Top-down 2D view of the building layout used for the case study.

5.3.2 Agents

Agents were placed throughout the building in a random manner while simultaneously placing the agents in as many rooms as possible, representative of a snapshot of how humans could be located at any given time within the building. The agents retain the same initial positions every time the simulation is run, as well as have an initial velocity of 0

m/s. Agents are given properties that correspond with default values for adults as specified in the FDS+Evac User Guide [52].

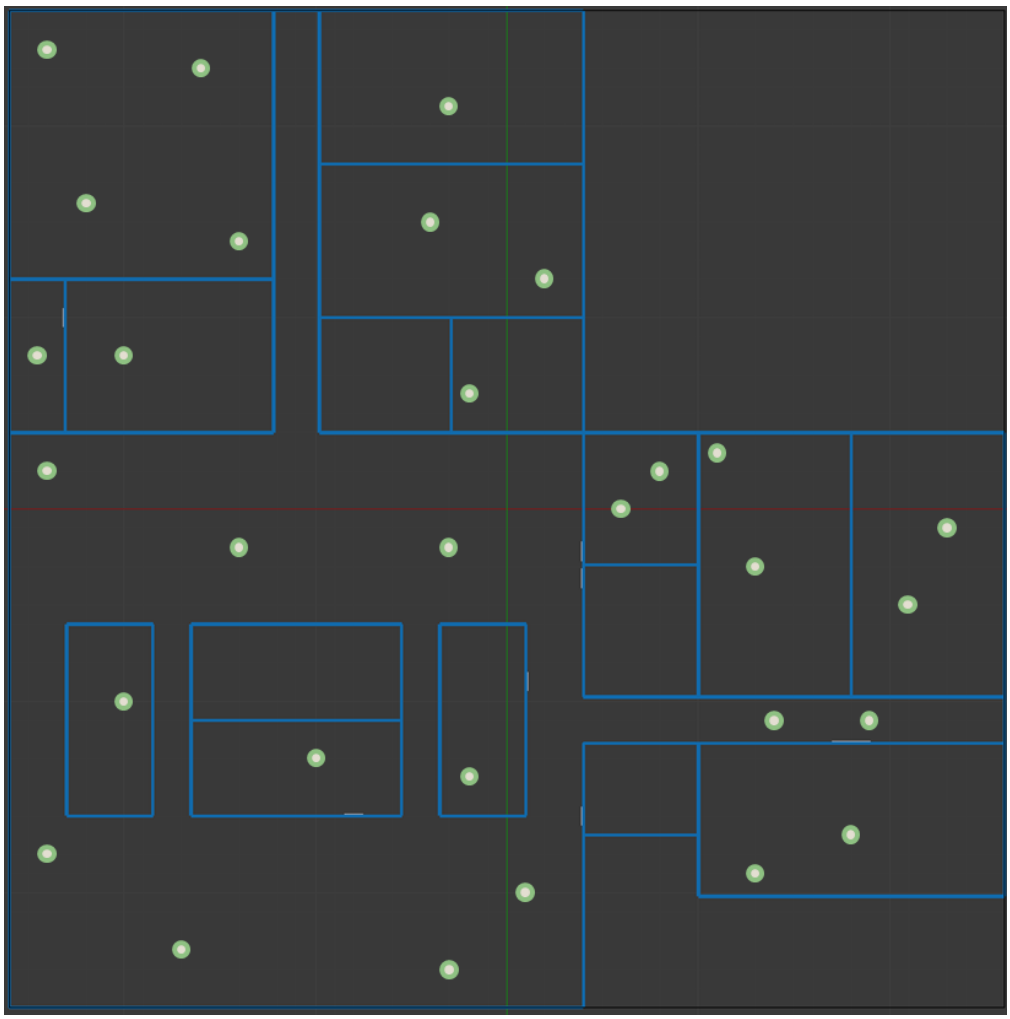

Figure 17 Schematic showing the initial positions of the agents.

5.3.3 Simulation Parameters

The evacuation scenario was simulated at different concentrations ranging from 0-600 ppm, in 100 ppm increments, with exceptions at 150 ppm and 450 ppm to observe thresholds in agent behavior. Agent properties set to the default values for adults. Social force model parameters are set as the default values within the FDS+Evac source code which are validated against other evacuation models and evacuation experiments [52]. Simulation end times were adjusted depending on how long the last agent would take to exit the geometry.

5.3.4 Simulation Results and Discussion

A notched box plot for distributions of agent evacuation times for different concentrations was plotted. The plot represents the exit data for all agents per simulation run, where the bottom whisker corresponds to the evacuation time of the first agent, while the top whisker corresponds to the evacuation time of the last agent. The bottom of the blue bar corresponds to the 25^{th} percentile, the top of the bar corresponds to the 75^{th} percentile, while the notch corresponds to the median evacuation time. Any agents that were incapacitated were considered to have an evacuation time of zero. An example of data along with labels is shown in Figure 18.

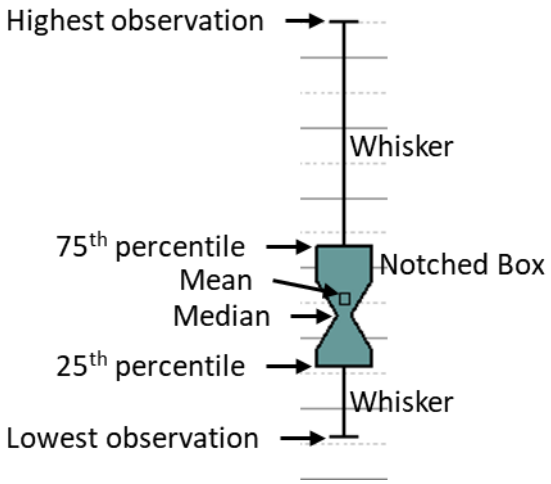

Figure 18 Illustration of data shown in notched box plots with labels.

The results of the case study are shown in Figure 19. The evacuation time of the last agent (denoted by the top whisker), as seen in Figure 19, is greatly affected by the concentration, as seen by its variation over the concentration range. The first agent's evacuation time (denoted by the bottom whisker) is shown to be largely unaffected by the exposure concentration.

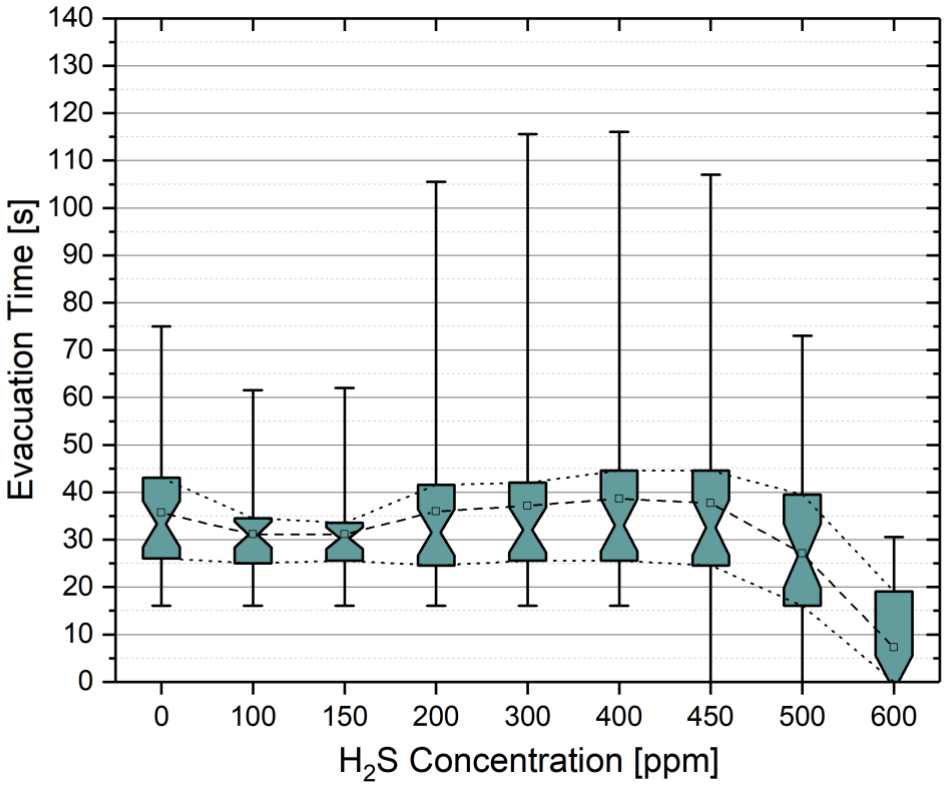

Figure 19 Notched box plot distribution of agent evacuation times for 30 agents at various concentrations.

Changing the concentration caused a small difference in the evacuation times of the 25th percentile of agents, followed by a more noticeable difference in the median evacuation time. The evacuation times of the 75th percentile of agents, however, are more affected by the concentration compared to the others. Interestingly, it can be seen that the evacuation times of the 25th percentile decrease as the concentration increases. This suggests that at least the first 25% of agents either do not exhibit eye and lung irritation (the 2nd symptom), or that their exposure is not long enough for the 2nd symptom to be sufficiently advanced

for their evacuation velocities to decrease below the unimpeded velocity. Agents that are incapacitated had their evacuation times recorded as zero, which skews the evacuation times of other percentiles downward. Because of this, the data distribution at concentrations where incapacitation is present (450 ppm and above) are not considered to be completely reliable. The only viable pieces of information in this concentration range are the evacuation times of the last able agents.

While this figure offers a somewhat comprehensive analysis of the evacuation scenario by showing the concentrations that cause agents to lose their ability to evacuate, it does not reveal certain aspects of the scenario. All things considered; the plot indicates that agents closest to the exits will be relatively affected by the toxic gas concentration. On the other hand, agents furthest from the exits are most affected by the toxic gas concentration, which is reflected in their variation in exit times and eventually their subsequent incapacitation. This analysis of evacuation times is insufficient when incapacitation is present. This arises due to several reasons. First, evacuation time paints an incomplete picture of the scenario. Evacuation time does not give any insight on the extent of toxic injury. Evacuation time is not an indicator of consequence, but more of an effect on the evacuation process caused by the consequence. Furthermore, evacuation time is not a useful metric when comparing the evacuation performance of two different building configurations in the light of evacuations in toxic environments. The data does not shed insight on what parts of the geometry are too far from exits that they may potentially result in agent incapacitation during evacuation. Finally, for the same building layout and gas concentration profile, the evacuation time is dependent on the initial position. This implies that one individual

scenario is not representative enough of the entire picture. Regardless, the figure highlights the importance of accounting for toxic effects under such evacuation scenarios.

Based on this, a contour mapping approach was proposed and conducted, tying the Toxic Load to the initial position of agents. This was done by first simulating 3 other evacuation scenarios, each with a different set of starting positions spread out in a way to ensure that a large portion of the geometry was covered.

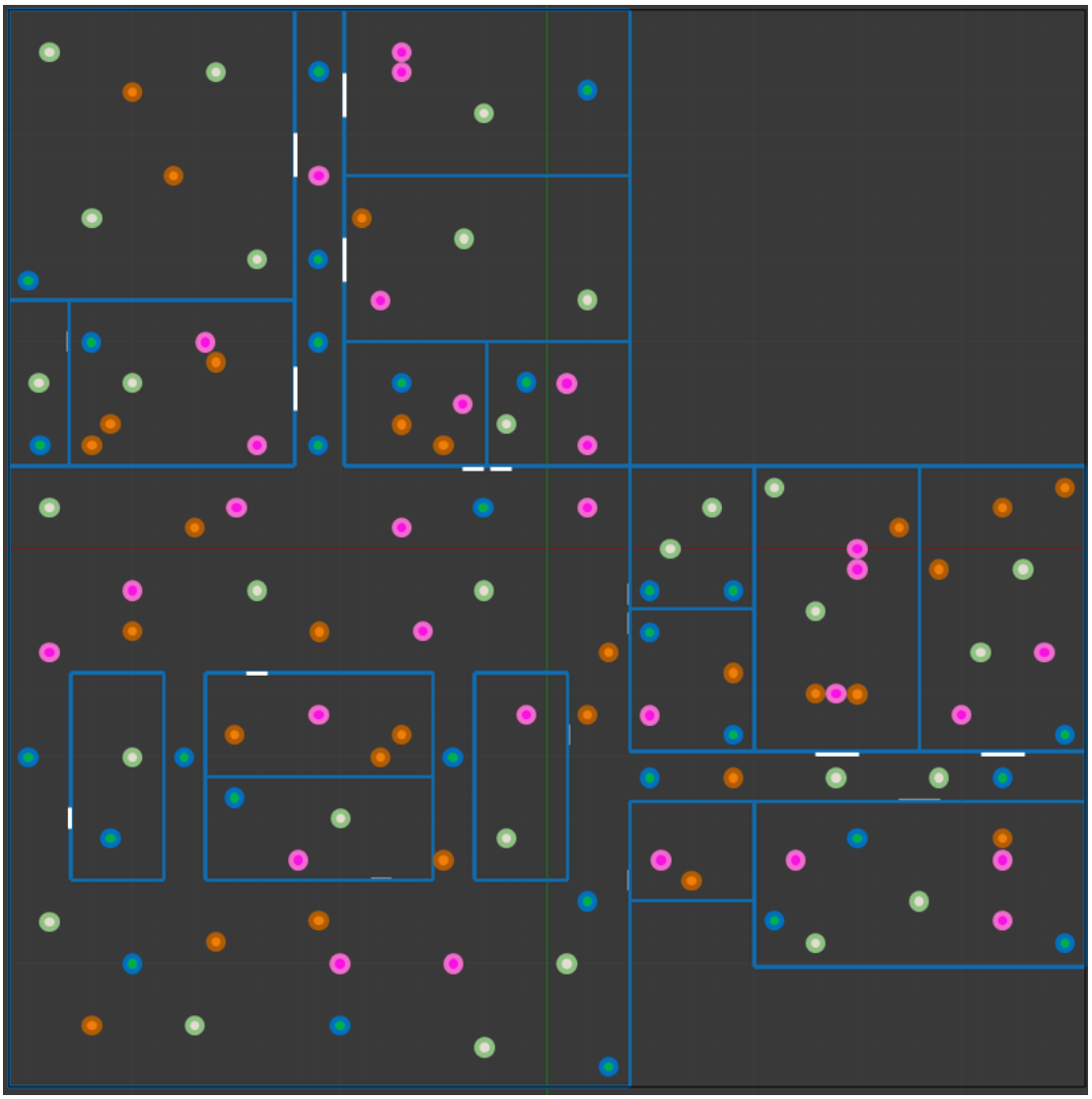

Figure 20 Schematic showing initial positions of the agents for each of the 4 runs.

Instead of recording agent evacuation times, the Toxic Load of each agent was recorded upon exit or incapacitation, and this was recorded alongside the initial starting position of each agent. The analysis was performed for concentrations in increments of 150 ppm between 150 and 600 to capture the various levels of Toxic Load as well as the

incapacitation threshold (450 ppm). A contour map was plotted from the results as shown in Figure 21 below.

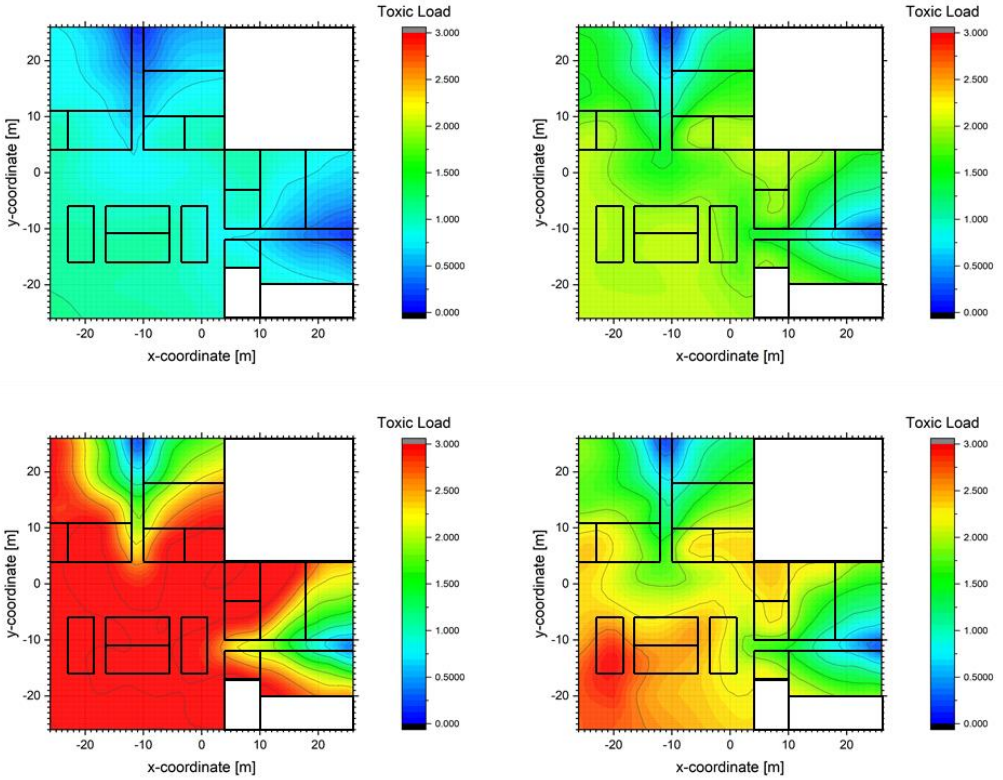

Figure 21 Contour plots of toxic load as a function of initial position at different H_2S concentrations. Starting from the top left, clockwise: 150 ppm, 300 ppm, 450 ppm, 600 ppm.

Figure 21 shows the expected Toxic Load (and therefore exposure symptom) that agents will experience depending on where they start evacuation. There are a few observations that can be made from looking at the plots. There is a characteristic contour shape resembling clogging/bottlenecking behavior at the start of the two long corridors. This demonstrates the plot's ability to evaluate the building's evacuation performance by

looking for certain markers that signify inefficient evacuation behavior. In addition, it shows the expected severity of exposure symptoms depending on how far agents are from the exits at a given concentration. Also, at the threshold concentration for incapacitation (450 ppm), it can be seen that the zone of concern involves the room near the bottom left corner of the building. This provides an assessment of the building in terms of evacuation performance that implies the need for a mitigation or emergency response strategy. For example, an emergency exit near the area would lessen the Toxic Load of agents evacuating nearby. The building configuration can also be modified to reduce the effects of clogging and bottlenecking Another possible solution could be the placement of self-contained breathing apparatus in the vicinity in the event of a toxic release incident. This demonstrates the usefulness of dosage contour maps as a consequence analysis tool for crowd evacuations in toxic environments, due to its ability to estimate the consequences of toxic exposure in a particular scenario, while pinpointing any weaknesses that a given building layout may potentially have.

The identification of these zones of concern shows the advantage of not only the use of a contour map, but also the advantage of accounting for toxic effects. The latter advantage can be shown by taking a similar contour mapping approach, but without accounting for toxic effects on the evacuation velocity and only carrying out dosage tracking. The side-by-side comparison of the two approaches are shown in Figure 22 below.

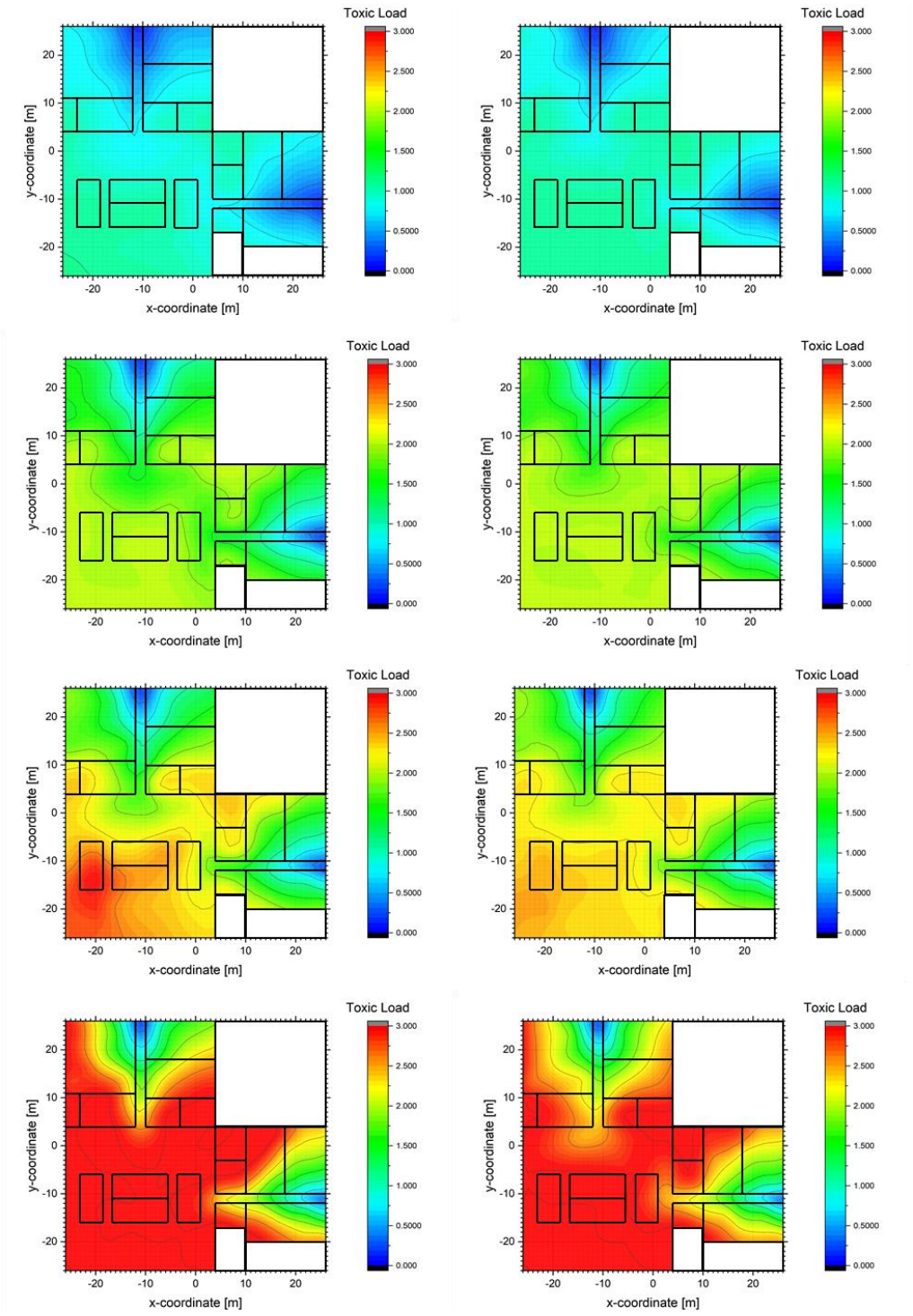

Figure 22 Comparison of Toxic Load contours when accounting for toxic effects (left) and not accounting for toxic effects (right) at different concentrations. Starting from the top, going down: 150 ppm, 300 ppm, 450 ppm, 600 ppm.

It can be seen from the figure that not accounting for toxic effects underestimates the size of the zones of concern. However, for this specific building layout, the difference between the two approaches is not very significant. It is expected that the difference between the two approaches will increase as the size of the building increases, due to there being longer evacuation paths. The difference is most significant at the incapacitation threshold, and this is due to the fact that accounting for toxic effects will always reach the incapacitation threshold concentration before the regular approach does. The difference is smaller at lower concentrations first due to the similarity in evacuation speeds as well as due to the fact that the loading rate is not significant enough to affect evacuation velocities. At these concentrations, toxic exposure has an insignificant impact on the evacuation process. Further beyond the incapacitation threshold, at 600 ppm, it can be seen that a large portion of the contour maps correspond to incapacitation of agents in either case. This is because the loading rate is high enough for agents to reach incapacitation whether their velocities are affected or not.

To further emphasize on the differences between modelling approaches and to provide more insights on the evacuation process, it is recommended to supplement the contour maps with frequency plots of Toxic Load to show the relative extent to which people are experiencing different levels of toxic injury.

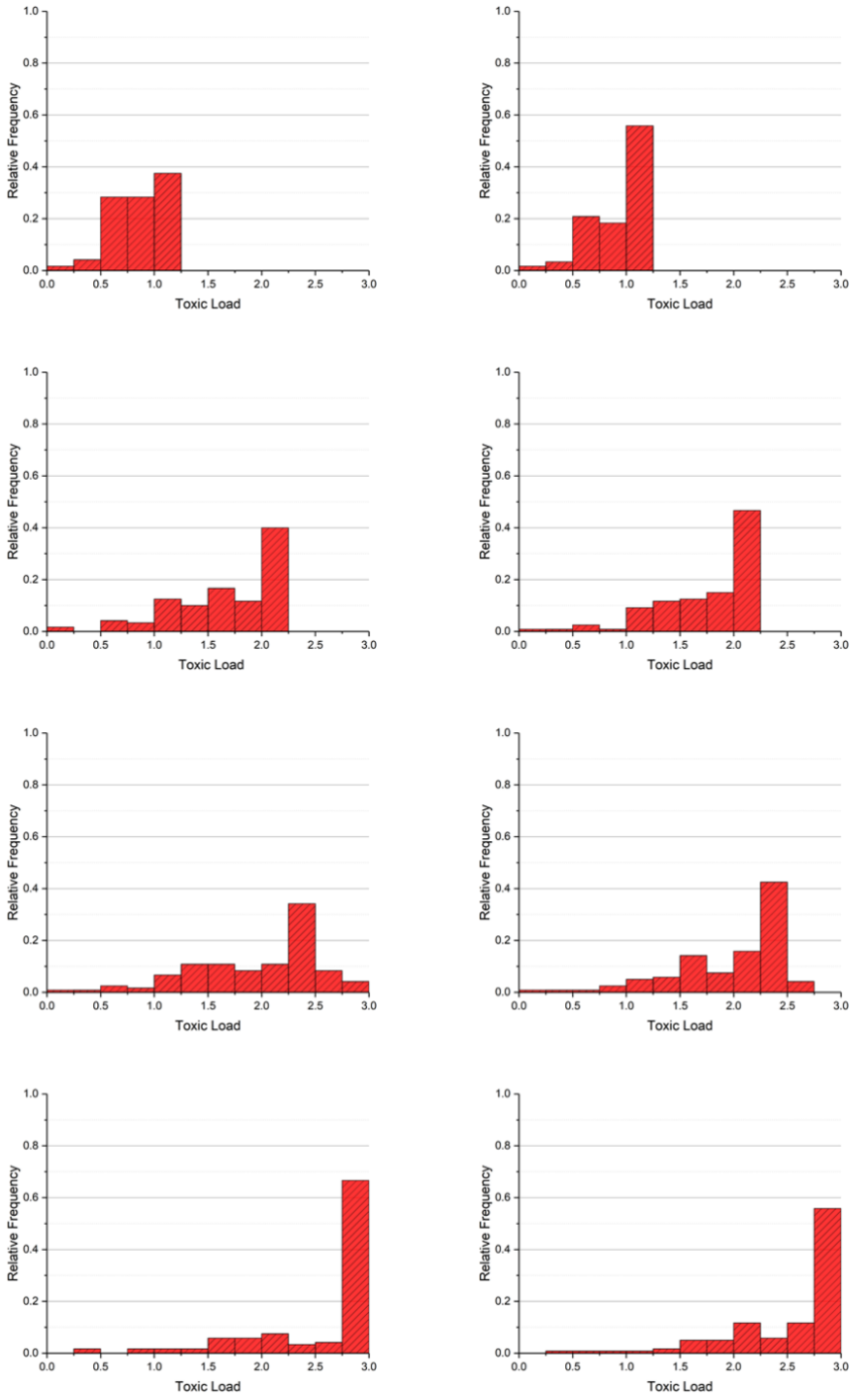

Figure 23 Comparison of Toxic Load frequency plots when accounting for toxic effects (left) and not accounting for toxic effects (right) at different concentrations. Starting from the top, going down: 150 ppm, 300 ppm, 450 ppm, 600 ppm.

Figure 23 shows that not accounting for toxic effects overestimates the dosage at lower concentrations. This is because of the panic symptom where agents move faster and thus have a lower time period of exposure. The figure also confirms incapacitation at 450 ppm when accounting for toxic effects, as opposed to not accounting for them.

6. CONCLUSIONS AND FUTURE WORK

This work covers the implementation of a dosage-based crowd evacuation methodology into a currently existing evacuation software tool used in real-life industrial applications. The implementation was followed by a case study and analysis to establish a contour mapping approach that provides a better visualization and understanding of the consequences that may arise during the evacuation process compared to reporting evacuation times and estimated number of fatalities which will vary from case to case. The contour mapping approach also has the potential to identify any aspects of a building's layout that might compromise the evacuation process in some way, rendering it a useful tool in the design process, such as the comparison of two different variations in the design of the same building. Furthermore, it can help with the planning of emergency response strategies such as the provision of breathing equipment or a well-coordinated evacuation plan. Well-coordinated evacuation plans can improve overall evacuation times by controlling evacuation panic that results in phenomena such as the "faster-is-slower" effect, and identification of problem areas within a building can allow for response planners to place breathing equipment nearby for quick emergency access.

The case study also highlights the importance of accounting for toxic exposure effects during evacuation, as shown by the methodology's ability to identify zones of concern within a building's layout. Additionally, it was able to anticipate a lower threshold concentration for incapacitation compared to an approach where toxic effects are not accounted for. The dosage algorithm in this study is versatile in that it can be applied in any building configuration for any toxic gas, given that the relevant information is

available. Furthermore, the methodology can readily accept new exposure-related data as more reliable toxicological data become available. An example of such data could be probabilistic exposure-response relationships, which addresses the heterogenous response to toxic exposure of individuals within a given population.

Further work should focus on incorporating more aspects of the FDS+Evac software into the approach. This involves complex processes such as the Computational Fluid Dynamics (CFD) model and an HVAC model that can both introduce complexity into the concentration profile of a toxic release. Additionally, more aspects of the evacuation simulation package can be included that can further diversify evacuation behavior in the form of diversified evacuation behavior (competitive, herding) as well as agent properties such as response time prior to evacuation. It is also recommended to study the effects of crowd density and its relative effect on the evacuation process, if any limiting behavior occurs as crowd density increases and social forces become more dominant.

One challenge faced by the methodology at its current state is the knowledge gap in terms of the direct effect of toxic gas exposure on peoples' ability to evacuate, both physically and psychologically. Currently available toxicological data relating symptoms to gas concentrations provide obscure definitions for time exposure, in addition to broad concentration ranges. There is little known on the psychological aspect of the evacuation process related to toxic exposure apart from vague definitions of panic and anxiety. Addressing these information gaps required some assumptions to be made.

However, the method of risk analysis highlighted in this study shows promise with the insight it provides in the areas of consequence analysis, emergency planning, and building design. Despite some imperfections in the simulation approach, it goes without saying that the implemented method of risk analysis will only be enhanced once a more comprehensive understanding of the evacuation process in toxic environments is reached.

REFERENCES

[1] E. Broughton, “The Bhopal disaster and its aftermath: A review,” *Environ. Heal. A Glob. Access Sci. Source*, vol. 4, pp. 1–6, 2005, doi: 10.1186/1476-069X-4-6.

[2] B. Eskenazi, M. Warner, P. Brambilla, S. Signorini, J. Ames, and P. Mocarelli, “The Seveso accident: A look at 40 years of health research and beyond,” *Environ. Int.*, vol. 121, no. June, pp. 71–84, 2018, doi: 10.1016/j.envint.2018.08.051.

[3] Z. Xiaoping, Z. Tingkuan, and L. Mengting, “Modeling crowd evacuation of a building based on seven methodological approaches,” *Build. Environ.*, vol. 44, pp. 437–445, 2009, doi: 10.1016/j.buildenv.2008.04.002.

[4] S. Wolfram, “Statistical Mechanics of Cellular Automata,” *Rev. Mod. Phys.*, vol. 55, no. July, pp. 601–644, 1983, doi: 10.1103/RevModPhys.55.601.

[5] Z. Daoliang, L. Yang, and L. Jian, “Exit dynamics of occupant evacuation in an emergency,” *Phys. A Stat. Mech. its Appl.*, vol. 363, pp. 501–511, 2006, doi: 10.1016/j.physa.2005.08.012.

[6] A. Varas, M. D. Cornejo, D. Mainemer, B. Toledo, and J. A. Valdivia, “Cellular automaton model for evacuation process with obstacles,” *Phys. A Stat. Mech. its Appl.*, vol. 382, pp. 631–642, 2007, doi: 10.1016/j.physa.2007.04.006.

[7] A. Kirchner, H. Klüpfel, K. Nishinari, A. Schadschneider, and M. Schreckenberg, “Simulation of competitive egress behavior: Comparison with aircraft evacuation data,” *Phys. A Stat. Mech. its Appl.*, vol. 324, no. 3–4, pp. 689–697, 2003, doi:

10.1016/S0378-4371(03)00076-1.

[8] A. Kirchner, K. Nishinari, and A. Schadschneider, “Friction effects and clogging in a cellular automaton model for pedestrian dynamics,” *Phys. Rev. E - Stat. Physics, Plasmas, Fluids, Relat. Interdiscip. Top.*, vol. 67, no. 5, p. 10, 2003, doi: 10.1103/PhysRevE.67.056122.

[9] W. Fang, L. Yang, and W. Fan, “Simulation of bi-direction pedestrian movement using a cellular automata model,” *Phys. A Stat. Mech. its Appl.*, vol. 321, pp. 633–640, 2003.

[10] Y. Tajima and T. Nagatani, “Scaling behavior of crowd flow outside a hall,” *Phys. A Stat. Mech. its Appl.*, vol. 292, no. 1–4, pp. 545–554, 2001, doi: 10.1016/S0378-4371(00)00630-0.

[11] D. Helbing, M. Isobe, T. Nagatani, and K. Takimoto, “Lattice gas simulation of experimentally studied evacuation dynamics,” *Phys. Rev. E.*, vol. 67, pp. 30–33, 2003, doi: 10.1103/PhysRevE.67.067101.

[12] W. Song, X. Xu, B. H. Wang, and S. Ni, “Simulation of evacuation processes using a multi-grid model for pedestrian dynamics,” *Phys. A Stat. Mech. its Appl.*, vol. 363, no. 2, pp. 492–500, 2006, doi: 10.1016/j.physa.2005.08.036.

[13] K. Lewin, *Field theory in social science*. 1951.

[14] D. Helbing and P. Molnar, “Social Force Model for Pedestrian Systems,” *Phys. Rev. E*, vol. 51, no. 5, pp. 4282–4286, 1995.

[15] D. Helbing, I. Farkas, and T. Vicsek, “Simulating dynamical features of escape panic,” *Nature*, vol. 407, no. 6803, pp. 487–490, 2000, doi: 10.1038/35035023.

[16] M. Zheng, Y. Kashimori, and T. Kambara, “A model describing collective behaviors of pedestrians with various personalities in danger situations,” in *ICONIP 2002 - Proceedings of the 9th International Conference on Neural Information Processing: Computational Intelligence for the E-Age*, 2002, vol. 4, pp. 2083–2087, doi: 10.1109/ICONIP.2002.1199043.

[17] C. M. Henein and T. White, “Macroscopic effects of microscopic forces between agents in crowd models,” *Phys. A Stat. Mech. Its Appl.*, vol. 373, pp. 694–712, 2007, doi: 10.1016/j.physa.2006.06.023.

[18] L. F. Henderson, “The Statistics of Crowd Fluids,” *Nature*, vol. 229, pp. 381–383, 1971.

[19] C. Mnasri and A. Farhat, “Numerical Simulation of the Flow of Crowds at the Jamarat Bridge during the Annual Hajj Event,” *Open J. Fluid Dyn.*, vol. 06, no. 04, pp. 321–331, 2016, doi: 10.4236/ojfd.2016.64024.

[20] R. L. Hughes, “The Flow of Human Crowds,” *Annu. Rev. Fluid Mech.*, vol. 35, no. 1997, pp. 169–182, 2003, doi: 10.1146/annurev.fluid.35.101101.161136.

[21] A. Braun, B. E. J. Bodmann, and S. R. Musse, “Simulating virtual crowds in emergency situations,” in *Proceedings of the ACM symposium on Virtual reality software and technology - VRST ’05*, 2005, p. 244, doi: 10.1145/1101616.1101666.

[22] X. Pan, C. S. Han, K. Dauber, and K. H. Law, “A multi-agent based framework for the simulation of human and social behaviors during emergency evacuations,” *AI Soc.*, vol. 22, no. 2, pp. 113–132, 2007, doi: 10.1007/s00146-007-0126-1.

[23] S. M. Lo, H. C. Huang, P. Wang, and K. K. Yuen, “A game theory based exit selection model for evacuation,” *Fire Saf. J.*, vol. 41, no. 5, pp. 364–369, 2006, doi: 10.1016/j.firesaf.2006.02.003.

[24] J. Guan, K. Wang, and F. Chen, “A cellular automaton model for evacuation flow using game theory,” *Phys. A Stat. Mech. its Appl.*, vol. 461, pp. 655–661, 2016, doi: 10.1016/j.physa.2016.05.062.

[25] C. Saloma, G. J. Perez, G. Tapang, M. Lim, and C. Palmes-Saloma, “Self-organized queuing and scale-free behavior in real escape panic,” in *Proc. Natl. Acad. Sci. 100*, 2003.

[26] A. Garcimartín, J. M. Pastor, L. M. Ferrer, J. J. Ramos, C. Martín-Gómez, and I. Zuriguel, “Flow and clogging of a sheep herd passing through a bottleneck,” *Phys. Rev. E - Stat. Nonlinear, Soft Matter Phys.*, vol. 91, no. 2, 2015, doi: 10.1103/PhysRevE.91.022808.

[27] A. Garcimartín, I. Zuriguel, J. M. Pastor, C. Martín-Gómez, and D. R. Parisi, “Experimental evidence of the ‘faster is slower’ effect,” *Transp. Res. Procedia*, vol. 2, pp. 760–767, 2014, doi: 10.1016/j.trpro.2014.09.085.

[28] E. Altshuler, O. Ramos, Y. Nunez, J. Fernandez, A. J. Batista-Leyva, and C. Noda,

"Symmetry breaking in escaping ants," *Am. Nat.*, vol. 166, pp. 643–649, 2005, doi: 10.1086/498139.

[29] M. Haghani and M. Sarvi, "Crowd behaviour and motion: Empirical methods," *Transp. Res. Part B Methodol.*, vol. 107, pp. 253–294, 2018, doi: 10.1016/j.trb.2017.06.017.

[30] C. H. Tang, W. T. Wu, and C. Y. Lin, "Using virtual reality to determine how emergency signs facilitate way-finding," *Appl. Ergon.*, vol. 40, no. 4, pp. 722–730, 2009, doi: 10.1016/j.apergo.2008.06.009.

[31] D. a C. F. L. Louvar, *Chemical Process Safety: Fundamentals with Applications*, 3rd Editio. Prentice Hall, 2011.

[32] H. Witschi, "Some notes on the history of Haber's law," *Toxicol. Sci.*, vol. 50, no. 2, pp. 164–168, 1999, doi: 10.1093/toxsci/50.2.164.

[33] D. W. Gaylor, "The use of Haber's Law in standard setting and risk assessment," *Toxicology*, vol. 149, pp. 17–19, 2000, doi: 10.1016/S0300-483X(00)00228-6.

[34] L. Stanley, E. Hanlon, J. Kelly, and B. Rayburn, "Potential Military Chemical/Biological Compounds," *Army Knowl.*, 2005.

[35] S. Mannan, *Lees' Loss Prevention in the Process Industries, Volumes 1-3*, 3rd Editio. Elsevier, 2005.

[36] W. F. ten Berge, A. Zwart, and L. M. Appelman, "CONCENTRATION--TIME

MORTALITY RESPONSE RELATIONSHIP OF IRRITANT AND SYSTEMICALLY ACTING VAPOURS AND GASES," *J. Hazard. Mater.*, vol. 13, pp. 301–309, 1986.

[37] J. P. Boris and G. Patnaik, "Acute Exposure Guideline Levels (AEGLs) for Time Varying Toxic Plumes," *Nav. Res. Labarotory*, vol. 30, p. 30, 2014.

[38] D. J. Ride, "A PRACTICAL METHOD OF ESTIMATING TOXIC LOADS IN THE PRESENCE OF CONCENTRATION FLUCTUATIONS," vol. 6, pp. 643–650, 1995.

[39] E. Yee, "Toxic Load Modeling for Naturally Fluctuating Concentration Exposures," no. May, 2013.

[40] AIHA Guideline Foundation, "2016 ERPG Introduction," 2016.

[41] National Research Council, *Acute Exposure Guideline Levels for Selected Airborne Chemicals, Volume 9*, vol. 9. 2010.

[42] HSE, "Methods of approximation and determination of human vulnerability for offshore major accident hazard assessment," 2013.

[43] N. Durak, M. Durak, E. D. Goodman, and R. Till, "OPTIMIZING AN AGENT-BASED TRAFFIC EVACUATION MODEL USING GENETIC ALGORITHMS," in *Proceedings of the 2015 Winter Simulation Conference*, 2015, pp. 288–299.

[44] J. Wan, J. Sui, and H. Yu, “Research on evacuation in the subway station in China based on the Combined Social Force Model,” *Phys. A Stat. Mech. its Appl.*, vol. 394, pp. 33–46, 2014, doi: 10.1016/j.physa.2013.09.060.

[45] R. Lovreglio, E. Ronchi, G. Maragkos, T. Beji, and B. Merci, “A dynamic approach for the impact of a toxic gas dispersion hazard considering human behaviour and dispersion modelling,” *J. Hazard. Mater.*, vol. 318, pp. 758–771, 2016, doi: 10.1016/j.jhazmat.2016.06.015.

[46] M. Liang, C. Bin, Q. Sihang, L. Zhen, and Q. Xiaogang, “Agent Based Modeling of Emergency Evacuation in a Railway Station Square Under Sarin Terrorist Attack,” *Int. J. Model. Simulation, Sci. Comput.*, 2016.

[47] S. M. Nawayd, “A Dosage Based Methodology to Simulate Crowd Evacuations in Toxic Environments,” Texas A&M University at Qatar, 2018.

[48] M. L. Chu, P. Parigi, J. C. Latombe, and K. H. Law, “Simulating effects of signage, groups, and crowds on emergent evacuation patterns,” *AI Soc.*, vol. 30, no. 4, pp. 493–507, 2015, doi: 10.1007/s00146-014-0557-4.

[49] S. Bae, J. H. Choi, C. Kim, W. hwa Hong, and H. S. Ryou, “Development of new evacuation model (BR-radiation model) through an experiment,” *J. Mech. Sci. Technol.*, vol. 30, no. 7, pp. 3379–3391, 2016, doi: 10.1007/s12206-016-0647-y.

[50] K. Fridolf, K. Andree, D. Nilsson, and H. Frantzich, “The impact of smoke on walking speed,” *Fire Mater.*, no. 2014, p. 4B, 2014, doi: 10.1002/fam.

[51] P. A. Thompson and E. W. Marchant, “A computer model for the evacuation of large building populations,” *Fire Saf. J.*, vol. 24, no. 2, pp. 131–148, 1995, doi: 10.1016/0379-7112(95)00019-P.

[52] T. Korhonen and S. Hostikka, “Fire Dynamics Simulator with Evacuation: FDS+EVAC - Technical Reference and User’s Guide (FDS 5.5.0, Evac 2.2.1),” 2015.

[53] J. Schmidt and A. Späh, “User Guide for Panic Simulator 1 . 0,” no. June, pp. 1–9, 2014.

[54] P. A. Langston, R. Masling, and B. N. Asmar, “Crowd dynamics discrete element multi-circle model,” *Saf. Sci.*, vol. 44, no. 5, pp. 395–417, 2006, doi: 10.1016/j.ssci.2005.11.007.

[55] Thunderhead Engineering, “Pathfinder Technical Reference,” *Capstone MicroTurbine*, pp. 1–23, 2014, doi: http://dx.doi.org/10.1046/j.1365-2796.2003.01129.x.

[56] World Health Organization Regional Office for Europe, “Air Quality Guidelines,” *J. Appl. Physiol.*, vol. 3, no. 2, pp. 1–7, 2007, doi: 10.1002/0471743984.vse4038.pub2.

[57] F. Danielsson, R. Fendler, M. Hailwood, and J. Shrives, “Analysis of H2S Incidents in Geothermal and other Industries,” *OECD Rep.*, 2009.

[58] S. Nogue, R. Pou, J. Fernandez, and P. Sanz-Gallen, “Fatal hydrogen sulphide

poisoning in unconfined spaces," *Occup. Med. (Chic. Ill).*, 2011.

[59] U.S. CSB, "Investigation Report, HYDROGEN SULFIDE POISONING," *U. S. Chem. Saf. Hazard Investig. Board*, 2003.

[60] M. Gorguner and A. Metin, "Acute inhalation injury," *Eurasian J. Med.*, vol. 42, pp. 28–35, 2010, doi: 10.5152/eajm.2010.09.

[61] Environmental Protection Agency, "Toxicological Review of Hydrogen Sulfide," 2003.

[62] T. L. Guidotti, "Hydrogen sulfide: Advances in understanding human toxicity," *Int. J. Toxicol.*, vol. 29, no. 6, pp. 569–581, 2010, doi: 10.1177/1091581810384882.

[63] T. L. Guidotti, "Hydrogen Sulphide," *Occup. Med. (Chic. Ill).*, vol. 46, no. November, pp. 367–371, 1982.

[64] Y. Bhambhani, R. Burnham, and G. Syndmiller, "Effects of 10-ppm Hydrogen Sulfide Inhalation on Pulmonary Function in Healthy Men and Women: Cardiovascular, Metabolic, and Biochemical Responses," *J. Occup. Environ. Med.*, vol. 38, pp. 1012–1017, 1996.

[65] Y. Bhambhani, R. Burnham, G. Syndmiller, I. Maclean, and T. Martin, "Effects of 10-ppm hydrogen sulfide inhalation in exercising men and women: cardiovascular, metabolic, and biochemical responses," *J. Occup. Environ. Med.*, vol. 39, no. 2, pp. 122–129, 1997, doi: 10.1097/00043764-199702000-00009.

[66] Y. Bhambhani and M. Singh, “Psychological Effects of Hydrogen Sulfide Inhalation on Healthy Exercising Men,” *Am. Psychol. Soc.*, 1991.

[67] Y. Bhambhani, G. Snydmiller, T. Martin, R. Burnham, and I. MacLean, “Comparative physiological responses of exercising men and women to 5 ppm hydrogen sulfide exposure,” *Am. Ind. Hyg. Assoc. J.*, vol. 55, no. 11, pp. 1030–1035, 1994, doi: 10.1080/15428119491018295.

[68] Y. Bhambhani, R. Burnham, G. Snydmiller, I. MacLean, and T. Martin, “Effects of 5 ppm hydrogen sulfide inhalation on biochemical properties of skeletal muscle in exercising men and women,” *Am. Ind. Hyg. Assoc. J.*, vol. 57, no. 5, pp. 464–468, 1996, doi: 10.1080/15428119691014819.

[69] N. Fiedler *et al.*, “Sensory and cognitive effects of acute exposure to hydrogen sulfide,” *Environ. Health Perspect.*, vol. 116, no. 1, pp. 78–85, 2008, doi: 10.1289/ehp.10531.

[70] J. Annegarn *et al.*, “Differences in walking pattern during 6-min walk test between patients with COPD and healthy subjects,” *PLoS One*, vol. 7, no. 5, pp. 3–8, 2012, doi: 10.1371/journal.pone.0037329.

[71] D. Stevens, E. Elpern, K. Sharma, P. Szidon, M. Ankin, and S. Kesten, “Comparison of Hallway and Treadmill Six-minute Walk Tests.”

[72] P. M. J. Swerts, R. Mostert, and E. F. M. Wouters, “Comparison of corridor and treadmill walking in patients with severe chronic obstructive pulmonary disease,”

Phys. Ther., vol. 70, no. 7, pp. 439–442, 1990, doi: 10.1093/ptj/70.7.439.

[73] Mayo Clinic Staff, "Pulmonary Edema," 2018. [Online]. Available: https://www.mayoclinic.org/diseases-conditions/pulmonary-edema/symptoms-causes/syc-20377009. [Accessed: 10-Jan-2019].

[74] OSHA, "Hydrogen Sulfide." [Online]. Available: https://www.osha.gov/SLTC/hydrogensulfide/hazards.html. [Accessed: 27-Dec-2018].

[75] H. Salem and S. A. Katz, *Inhalation Toxicology*, 3rd ed. CRC Press, 2016.

[76] N. M. Shaikh, K. E. Kakosimos, N. Adia, and L. Vechot, "Concept and demonstration of a fully coupled and dynamic exposure-response methodology for crowd evacuation numerical modelling in airborne-toxic environments," *J. Hazard. Mater.*, vol. 399, no. May, 2020, doi: 10.1016/j.jhazmat.2020.123093.